Expedited screening of methanotroph-microalgae cocultures for integrated biogas valorization and wastewater remediation

Loyal P. Murphy, Q. Peter He, Jin Wang*

Department of Chemical Engineering, Auburn University, Auburn, AL 36849

Correspondence Author: wang@auburn.edu

Abstract:

Anaerobic digestion (AD) is a well-established waste-to-value technology commonly used at water resource recovery facilities (WRRFs), generating biogas from organic waste. However, the generated biogas is typically used only for heat and electricity generation due to contaminants, while the nutrient-rich AD effluent requires further treatment before environmental release. Methanotroph-microalgae cocultures have recently emerged as promising candidates for integrated biogas valorization and nutrient recovery. Although the choice of the coculture pairs is one of the most important factors that determine the performance of the application, there have not been any results on the comparison or screening of different coculture pairs for a desired application. To expedite the screening of methanotroph-microalgae cocultures for optimal performance, we developed a cost-effective screening system consisting of nine parallel bioreactors. The compact design of the system allows it to fit in a fume hood, and enables the simultaneous evaluation of multiple species with triplicates under uniformly controlled conditions. The system was applied to screen seven methanotrophs, five microalgae, and six methanotroph-microalgae coculture pairs on a diluted AD effluent from a local WRRF. To systematically assess the growth performance of different monocultures and cocultures, mathematical models that describe the microbial growth under batch cultivation were developed to determine the maximum growth rate, delay time, and carrying capacity from growth data, allowing for consistent and systematic assessment of different species, as well as the identification of the coculture pairs with synergistic and inhibitory interactions. The developed experimental system and modeling approach enabled expedited strain screening and unbiased assessment for integrated biogas valorization and nutrient recovery. Specifically, the cost of each bioreactor system in S3 is less than 5% of commercially available bioreactor system (such as Bioflo 120), while the screening throughput of S3 is 9 times that of a single bioreactor system. In addition, the identified synergistic cocultures demonstrate potential for scalable biogas valorization and nutrient recovery in wastewater treatment.

Keywords:

Biogas valorization, nutrient recovery, methanotroph-microalgae coculture, inter-species metabolic interactions, anaerobic digestion, modified Gompertz model, expedited screening

1) Introduction:

Municipal, agricultural, and industrial processes produce large amounts of wastewater that has caused detrimental impacts on the environment and local communities. In addition, wastewater is the fifth largest anthropogenic source of methane emissions globally, with US wastewater alone producing 20.8 million metric tons of CO_2 equivalent (CO_2e) in 2022 (U.S. Environmental Protection Agency, 2024). AD is commonly regarded as the most effective waste management solution for wet organic waste and is currently the only widely commercialized waste-to-value (W2V) process at scale. In anaerobic digesters, microbial communities break down organic matter into biogas (about 60% CH_4 and 40% CO_2, with trace amounts of other gases such as H_2S), and nutrient-rich digestate (containing valuable elements such as N, P, and K). Furthermore, AD is highly effective at mitigating odors and pathogens (Angelidaki and Ellegaard, 2003; Nasir et al., 2012; Topper et al., 2006). Given its many environmental benefits, AD has been widely adopted by large-scale WRRFs. In the US, 48% of total wastewater flows are treated by AD, with at least 1238 WRRFs (out of 14,780 WRRFs in the US) processing solids through AD (Qi et al., 2013).

Many W2V technologies could utilize AD as a key process(Patel et al., 2023). The two most prominent ones are: (1) combined heat and power (CHP), which utilizes AD-produced biogas to generate heat and/or electricity; and (2) Renewable natural gas (RNG) or biomethane (BM), where AD-produced biogas is upgraded to meet pipeline quality standards to be used as a transportation fuel or injected into natural gas pipelines (Wang and He, 2023). Despite their wide recognition, there are challenges associated with these technologies. For example, both CHP and BM require significant capital expenditure (CapEx) and operating expenses (OpEx) due to the impurities in biogas (*e.g.*, H_2S and NH_3). In addition, the low-value products (electricity, heat, or methane) further deteriorate their economic viability. As a result of poor return on investment (ROI), both CHP and BM have limited success in the US. For example, among the WRRFs with AD installed, 15% (~184) of them flare the produced biogas, 64% (~791) of them burn the biogas for digester and building heating, while only 21% (~263) of them use biogas for power generation or driving machinery (Qi et al., 2013).

Recently, it has been demonstrated that methanotroph-microalgae cocultures offer a highly effective platform for biogas valorization and nutrient recovery from wastewater. Methanotrophs are microorganisms that utilize methane (under atmosphere pressure and temperature) as their sole carbon and energy source to grow. Aerobic methanotrophs require oxygen to oxidize methane and exhibit higher growth rates than anaerobic methanotrophs. Although biogas is rich in methane, it does not contain the oxygen required by the aerobic methanotroph to grow. It has been reported that the coupling of methane oxidation (by methanotrophs) and oxygenic photosynthesis (by photoautotrophs or plants) is prevalent in nature to reduce CH_4 emissions and reuse CO_2 (Kip et al., 2010;

Milucka et al., 2015; Raghoebarsing et al., 2005). The metabolic coupling of methane oxidation and photosynthesis offers many advantages for biogas valorization. First, the exchange of *in situ* produced O_2 and CO_2 dramatically reduces mass transfer resistance of the two gas substrates; (2) *in situ* O_2 consumption removes inhibition on photoautotroph and eliminates the risk of explosion; (3) interdependent yet compartmentalized configuration of the coculture offers flexibility and more options for metabolic engineering; (4) there may be other metabolic interactions that could promote the growth of both species. Exploring the synergistic relationship between methanotrophs and microalgae, several groups have demonstrated that methanotroph-microalgae cocultures can significantly increase biomass production and nutrient recovery for wastewater treatment (Badr et al., 2022; Rasouli et al., 2018; Roberts et al., 2020; Wang et al., 2022; Zhang et al., 2023).

The methanotroph-microalgae coculture converts the carbon contained in both CH_4 and CO_2 into biomass, which can serve as feedstock for animal feed or bioplastic production (Wang and He, 2023). Although methanotrophs can convert methane into different chemicals such as methanol, lactic acid, etc. (Patel et al., 2023), the required downstream processing to separate and purify the low-concentration products often deteriorates the economic feasibility of the overall process. In this work, we focus on producing biomass as the desired product, as the simple downstream processing involved for animal feed or bioplastic production (drying and extrusion) requires limited capital and operational cost, while producing a value-added product (animal feed or bioplastics). In addition, the coculture based approach does not require extensive pretreatment to remove impurities, as one can choose the coculture pairs that can tolerate high concentrations of impurities (H_2S and/or NH_3) (Roberts et al., 2020). Therefore, the methanotroph-microalgae coculture based approach offers great potential for a sustainable, profitable and effective W2V technology.

The choice of the biocatalyst, i.e., the methanotroph-microalgae coculture, has arguably the biggest impact on the performance of the coculture W2V platform. The ideal biocatalysts should be able to tolerate various inhibitors in the AD digestate and raw biogas, while delivering robust and stable growth under various disturbances, such as light intensity, light-dark cycle, and availability of macro- and micro-nutrients (*e.g.*, N and P). Our prior research has shown that not all methanotroph-microalgae pairs form a synergistic partnership, even if they can grow together (Roberts et al., 2020). Therefore, screening different methanotrophic and microalgae strains is necessary to optimize carbon and nutrient recovery. However, existing research on methanotroph-microalgae cocultures all focused on the performance of selected coculture pairs in biogas conversion or biomass production. There has not been any report on a comprehensive comparison or screening of different species. In addition, there is a lack of quantitative evaluation on the effect of interspecies interactions within a given coculture. These are likely due to the challenges associated with characterizing and studying mixed culture or

microbial communities (Badr et al., 2022, 2021). Meanwhile, the screening of different coculture pairs is a time- and labor-intensive process. To ensure consistent growth conditions during the screening of different strains, bioreactors with continuous control of various abiotic factors such as pH, temperature and gas feeding rate are preferred. Given the number of methanotrophic and microalgae species n_1 and n_2, there are $3\times n_1\times n_2$ potential coculture screening runs to be conducted (assuming triplicates for each pair) using a single bioreactor.

To speed up the screening process in terms of throughput and cost-effectiveness, we have developed specialized equipment, termed species screening system (S3), consisting of nine parallel bioreactors. The compact design of the system allows it to fit in a fume hood and enables the simultaneous evaluation of multiple species with triplicates under uniformly controlled conditions. Using S3, seven methanotrophs, five microalgae and six methanotroph-microalgae coculture pairs were screened. To quantitatively and systematically evaluate the growth performance of different single cultures and cocultures, we developed a mathematical model to capture the key growth characteristics of different species, including growth delay, maximum growth rate, and carrying capacity. The performance of different species or coculture pairs are evaluated consistently using the estimated growth characteristics. Finally, we used the screening system to examine the effect of temperature on both monoculture and cocultures. The nine parallel bioreactors significantly expedited experimental execution for strain screening. In addition, the mathematical model not only provides a framework for unbiased evaluation of different coculture pairs but also allows the identification of interspecies interactions within different coculture pairs.

2) Materials and methods

2.1) Wastewater Acquisition and Preprocessing

AD digestate, i.e., liquid effluent from a mesophilic AD, was collected from the South Columbus Water Resource Facility (Columbus Water Works, Columbus, Georgia, USA). In addition, clarifier water was also collected to dilute the AD digestate. All liquid samples were transported on ice from the facility to the laboratory, where they were stored at -20°C until needed.

For the screening experiment, the AD digestate and clarifier water were thawed at 4°C for roughly 24 hours. The liquid samples were decanted, centrifuged (4400rpm, 10mins, 22°C), and vacuum filtered (polyethylsulfone, 0.2 μm pore-size) to remove large particulates and other microbes. After these preprocessing steps, the AD digestate was mixed with filtered clarifier water to obtain diluted AD digestate, which contains 10 vol% digestate and 90 vol% clarifier water for screening (which is termed 10% digestate).

2.2) Strain and cultivation

Seven methanotrophs and five microalgae were examined in this work. The species, preculture medium, and cultivation conditions (i.e., temperature and feeding gas composition) are listed in **Table 1**. The methanotrophs examined in this work include five Type I, one Type II, and one Type X methanotrophs. Two genera of microalgae (*Chlorella* and *Scenedesmus*) were included in this study.

[insert Table 1 here]

For each species, thawed frozen stock was washed twice with its corresponding defined medium as listed in **Table 1** and inoculated into 30 mL of the same medium (which is termed frozen inoculum). The frozen inoculum was cultivated at its optimal temperature and initial pH at 200 rpm. Once the frozen inoculum reached the early exponential phase when the optical density (OD) reached about 0.5 (Beckman Coulter UV-VIS Spectrophotometer DU1800, California, USA), about 10 ml of the culture broth was transferred to the preculture medium, which is a 1:1 mixture of 10% digestate and defined medium. This preculturing step provides an adaptation period for the species to get accustomed to the inhibitors in the AD digestate. Once the preculture reached its mid-exponential phase with an OD of around 1.0, it was used to inoculate the S3 vials containing 10% digestate at an initial OD of around 0.08.

2.3) Species Screening System (S3)

The S3 is a multi-bioreactor system we developed in-house to expedite the screening of different strains. It consists of nine parallel batch bioreactor systems made of 500 mL cylindrical glass vials. Each vessel is capped with a rubber stopper to maintain an airtight seal. Each robber stopper contains six ports to hold a temperature probe, pH probe, three separate 316 stainless steel tubes for acid/base addition, inlet and outlet gas, and one septum for liquid sampling. A vessel schematic is provided in Supplementary Material **Figure S1**.

Each vessel is placed on a Four E's scientific stir plate (Guangzhou, China) to regulate temperature and agitation, and equipped with a BlueLab pH controller (Bay of Islands, New Zealand). In addition, two parallel LED walls were crafted using cool white LEDs from HitLights (Louisiana, USA) with adjustable faders that illuminate all nine reactor systems. Mirrors and additional LEDs were added to ensure that the edges received adequate light, as illustrated in Supplementary Material **Figure S2**.

Ultra-high purity CH_4, O_2, N_2, and bone-dry CO_2 (Airgas, USA) were mixed to generate the feeding gas for different strains. Each gas cylinder was equipped with an Alicat Scientific (Arizona, USA) mass flow controller (MFC) to ensure consistent feed gas composition. Gases from the MFCs were driven through a static mixer followed by a nine-way manifold. Each outlet from the manifold was equipped with a variable-area gas flow meter from Cole-Parmer (Illinois, USA) to equilibrate the resistances among all nine vessel inlet lines. These flow meters ensured the feeding gas into each reactor system had an

equivalent volumetric flow rate. The gas schematic setup is illustrated in Supplementary Material **Figure S3**.

2.4) Validation of S3

Chlorella sorokiniana was cultivated in all nine vessels on 10% digestate to validate the consistency among different reactor systems. The inoculum was prepared following the protocol detailed in *Section 2.2*. The strain was cultivated on S3 for 120 hours under the following growth condition: 28°C, 300 rpm, 0.22 vvm of 2 vol% CO_2 in N_2, pH of 7.0, and 180 μE/m^2/s. The OD of each vial was measured 3-4 times per day to track the growth of microalgae and evaluate the consistency of the nine reactor systems.

2.5) Monoculture Screening

The monocultures of seven methanotrophs and five microalgae were screened on 10% digestate in triplicate on the S3. For each strain, its preculture was inoculated into 250mL of 10% digestate to achieve an initial OD of 0.080 ± 0.010 at 600nm for methanotrophs and 750nm for microalgae. The same growth conditions listed in **Table 1** for preculture preparation were used for the S3 screening. Liquid samples were taken 3-4 times daily to track growth progress through UV-Vis wavelength scans from 400nm – 800nm. Aside from *Methylosarcina quisquiliarum*, all strains were allowed to grow until reaching the late-exponential phase.

In addition to biomass, total nitrogen and total phosphorus were quantified with Hach chemistry kits (TNT826 and TNT844, Colorado, USA) at the beginning of, and 24 or 48 hours into, the experiment, depending on the delay time. Specifically, liquid samples were centrifuged at 15,000rpm for 10 minutes, then the supernatant was analyzed following the instructions of the Hatch kits.

2.6) Coculture Screening

Three methanotroph and two microalgae strains were selected for coculture screening, based on the monoculture screening result. A full factorial design results in six coculture pairs to be screened. For each coculture pair, the preculture of individual strain was prepared as described in *Section 2.2* and inoculated into 250mL of 10% digestate. The coculture inoculum had an initial OD at 750nm of 0.080 ± 0.010, with the initial dry cell weight ratio between the microalgae and the methanotroph of 4:1. The growth conditions for each pair were listed in **Table 1**.

During the screening experiments, liquid samples were taken 3-4 times per day, and the OD wavelength scans from 400nm – 800nm were collected. To determine the coculture biomass concentration, 1mL of well-mixed coculture broth was dried for 24 hours at 70°C. To account for the weight of involatile solids in 10% digestate, this drying protocol was repeated with just 10% digestate, and the weight of the involatile solids was subtracted from the dried broth samples.

2.7) Temperature effect of *Methylococcus capsulatus* and its Cocultures

To study the effect on *M. capsulatus* monoculture, the same protocol described in *Section 2.5* was followed, with different temperatures of 30°C, 37°C, 42°C, or 47°C. Similarly, *M. capsulatus* coculture trials were conducted following protocols described in *Section* 2.6, with the screening temperature adjusted to either 30°C or 37°C. For the coculture temperature screening, at the end of each trial, a microscope image of an undiluted sample at 40x magnification was taken.

2.8) Modified Gompertz Model (4Z Model)

Gompertz model has been widely used for modeling microbial growth because it effectively describes the sigmoidal (S-shaped) growth curves of batch experiments. In addition, unlike Monod model, Gompertz model does not require substrate concentrations to estimate model parameters. It only requires sequential biomass concentration measurements to estimate key model parameters. Similar to the logistic model, Gompertz is capable of capturing microbial growth dynamics under limited resources (nutrients and/or substrates), while offering additional flexibility with three model parameters compared to the logistics model (with two model parameters).

In this work, we introduce a modified Gompertz model to capture the entire biomass growth trajectory during the screening experiment. The modified Gompertz model was based on the Zwietering modification of the original Gompertz model (Tjørve and Tjørve, 2017; Zwietering et al., 1990), with a constant term added to address the discrepancy between model prediction and measurements of initial biomass concentration. The modified Gompertz model is given below:

$$X(t) = K\exp\left(-\exp\left(\frac{e*\mu_{rel}}{K}\left(T_{lag} - t\right) + 1\right)\right) + X_o. \quad (1)$$

where X_o, t and $X(t)$ denote the initial biomass concentration (gDCW/L), time (hr), and biomass concentration at time t, respectively. K, μ_{rel}, T_{lag} are model parameters to be estimated using $X(t)$. Given that the minuscule initial biomass measurement may be susceptible to higher uncertainty, the X_o parameter was also given partial flexibility between 70% and 130% of the initial biomass measurement. K (gDCW/L) denotes the carrying capacity, i.e., the maximum biomass concentration that could be reached in the stationary phase; μ_{rel} (1/hr) denotes a certain growth rate that is relevant to but not equal to the maximum growth rate commonly used in the Monod model; T_{lag} represents "the time between when a microbial population transferred to a new habitat recovers and when a considerable cell division occurs" (Tjørve and Tjørve, 2017; Zwietering et al., 1990). Including X_o, there are four parameters in the modified Gompertz model, which is referred to as the 4Z model.

As shown in the Results section, the 4Z model can adequately capture the batch growth profiles of all monocultures and all coculture pairs except for *Methylosarcina fibrata – Chlorella sorokiniana*. However, the parameters of the 4Z model are not directly related to the parameters commonly used to characterize cell growth, such as maximum growth rate and delay time. To enable easy assessment of different strain's growth performance, we developed the following procedure to determine the maximum growth rate and delay time used in the exponential growth from the parameters of the 4Z model.

The exponential growth model, shown in Eqn. (2), describes the unlimited growth of a microbe.

$$X(t) = X_o \exp(\mu_{max}(t - t_d)) \text{ for } t \geq t_d \quad (2)$$

where μ_{max} (1/hr) represents the maximum growth rate and t_d (hr) represents the delay time. As the exponential growth model applies to the initial period of batch growth when cell growth was unlimited, only the first few measurements are suitable for fitting the model. As a result, the limited number of and the errors contained in the first few biomass concentration measurements (which were all quite small) could cause biased estimates of the model parameters. To address this limitation, we used the biomass concentration predicted by the fitted 4Z model over the time range $[0, T_{lag}]$ to estimate μ_{max} and t_d. In this way, the 4Z model estimated from the full growth trajectory is applied to estimate the biologically significant parameters μ_{max} and t_d. This approach enables robust and unbiased estimation of μ_{max} and t_d rather than estimating them using the few initial measurements of a batch growth experiment.

Detailed description and MATLAB live scripts for the modified Gompertz model and data analysis can be found in the accompanying Method X paper: "A Modified Gompertz Model and Its MATLAB Implementation for Microbial Growth Performance Assessment."

3) Results and Discussion

In this work, the individual species were selected with a focus on their feasibility for wastewater treatment. Of the five Type I methanotrophs, both *Methylomonas* and *Methylosarcina* genera have shown robust growth in synthetic and authentic wastewater (AlSayed et al., 2018; Kim et al., 2018). In addition, *Methylosinus trichosporium* OB3b is a model methanotroph and has been studied extensively for its potential to produce carboxylic acids for renewable plastics and versatility in copper-rich and copper-deficient environments(Nguyen et al., 2020; Zhang et al., 2017). Lastly, the Type X *Methylococcus* capsulatus (Bath) is another model methanotroph and, to our knowledge, is the only methanotroph used in industrial applications (Liu et al., 1997; Ward et al., 2004). For the microalgae candidates, *Chlorella* and *Scenedesmus* species were selected for their extensive application and robust growth in wastewater remediation (Gupta et al., 2016; Wollmann et al., 2019).

In the S3 setup, the supply of carbon substrate (CH_4 and CO_2) is unlimited through continuous bubbling of the feed gas through the vessel. The supply of macronutrients (N, P, etc.) is through the diluted AD digestate, which is limited. In this work, we primarily consider the growth performance of each candidate as metrics for screening due to the following considerations: first, our prior work showed that the removal of N and P from wastewater is linearly proportional to the biomass production before the nutrient in the culture medium is depleted (Roberts et al., 2020). In addition, all strains screened in this work fully removed the inorganic nitrogen and phosphorus from the AD digestate within the first 48 hours.

Directly comparing the growth profile of each strain can be subjective and lead to biased conclusions, as different species exhibit different delay times and growth characteristics. To minimize the potential bias, we use parameters obtained from fitting the growth data to the modified Gompertz model (i.e., the 4Z model) to quantitatively evaluate each strain for its potential in the desired application. Specifically, we compare the maximum growth rate, the delay time and the carrying capacity exhibited by each monoculture or coculture to assess their potential in the application of integrated biogas valorization and wastewater treatment. As N/P removal is linearly correlated to biomass production, the maximum growth rate (exhibited in the early exponential growth phase) serves as a good indication of how efficient the strain is in nutrient recovery and biomass production. In addition, a strain's delay time indicates how robust the strain is when exposed to various inhibitors in the wastewater. A short delay time is desired as the inhibitors contained in the wastewater change frequently over time. In addition, a short delay time indicates a smaller bioreactor can deliver the same throughput. Finally, as the produced biomass serves as a co-benefit, which is the feedstock for animal feed or bioplastic production, the carrying capacity indicates how much biomass can be produced with limited nutrients in the liquid phase (carbon supply from the continuous gas phase is unlimited in the screening). Therefore, it is desirable to maximize biomass production in addition to prioritizing fast growth and short delay time.

3.1) S3 development and validation

The development of the S3 was driven by the need for an affordable and effective system that can expedite the biological screening of different methanotroph-microalgae cocultures. Therefore, the S3 is expected to deliver tightly controlled growth conditions across different parallel reactor systems in a cost-effective way. In addition to the culture medium, the most important abiotic factors involved in methanotroph, microalgae, and coculture cultivation are temperature, pH, agitation rate (which determines the mass transfer rate of the gas substrate), gas feed rate, gas composition, and light intensity (for microalgae and the coculture). Below we briefly discuss how the S3 delivers consistent growth conditions across the nine parallel reactor systems.

Temperate is controlled by the stir plate underneath the glass vessel with a precision of ± 1 °C. pH is controlled through the pH controller, with a precision of ± 0.1. The agitation rate is controlled by the stir plate as well, with a precision of ± 50 rpm, which is not ideal. However, as the purpose of controlling the agitation rate is to achieve the same mass transfer rate across different vessels, we address this limitation by setting the agitation rate at 300 ± 50 rpm, where the variation in agitation has little effect on mass transfer. In terms of controlling feed gas composition and feed gas flow rate, we use a combination of highly accurate mass flow controllers (with flow rate accuracy of ± 1 smL/min) and affordable variable area flow meters as described in *Section 2.3*. Finally, to maintain the uniform photon distribution across all nine vessels, we used two LED walls that face the nine vessels as the light source, with mirrors and additional LED sources installed at both ends. The light intensity across all nine systems has a precision of ± 2μE/m^2/s for a target of 180μE/m^2/s. A picture of the fully equipped S3 is given in **Figure 1a**.

[insert Figure 1 here]

S3 was designed to be cost-effective while ensuring its performance. For example, variable area flow controllers (~ $100 each) are used to evenly distribute gas supply to all nine vessels while MFCs (~ 1000 each) are chosen to regulate the gas composition and total gas supply to S3. In addition, the choice of the pH controller and stir plates (for temperature and agitation control) were also based on performance and affordability, with the selection of operation conditions to compensate for the lack of accuracy in agitation control. The total cost for the nine-vessel S3 system was less than $8,000 (with each bioreactor system cost less than $900). If a commercial bioreactor system is used, such as Bioflo 120 (Eppendorf, USA), the cost for one bioreactor (including pH and temperature control) is about $20,000. With the nine parallel bioreactor system, S3 can improve the screening throughput by 9-fold.

To validate that the S3 delivers consistent growth conditions across all nine reactor systems, *Chlorella sorokiniana* was grown on the S3 for 120 hours. **Figure 1b** plots the biomass concentration over time for all nine vessels. Throughout the screening, biomass measurement at each time point had a standard deviation of less than 5% of its respective value. This result indicates that different reactor systems delivered consistent growth conditions, which enabled the uniform growth performance of the same strain across all nine vessels.

To quantitatively evaluate the consistency among the nine vessels, we conduct statistical tests on the *C. sorokiniana* growth data. In this experiment, we have obtained 13 measurements of OD (then converted to DCW) over time for a period of ~120 hours. Since cell growth measurements were recorded on the same subject (*i.e.*, *C. sorokiniana* in the vial) repeatedly over time, it is inappropriate to use the standard analysis of variance (ANOVA) method to compare group means, as it does not consider dependencies among measurements within subjects. To address this challenge, we applied repeated measures

ANOVA or RM-ANOVA (Girden, 1992) for statistical testing. Repeated measurements refer to the biomass measurement of *C. sorokiniana* obtained at different times. RM-ANOVA is suitable for time-series data because it is designed to analyze data where the same subjects are measured multiple times under different conditions and/or over time. Because we are less interested in time as a factor, which has been thoroughly investigated by mathematical modeling, other time-series specific modeling techniques, such as autoregressive integrated moving average (ARIMA), are not used. To perform RM-ANOVA, we divide the nine bioreactors into three groups based on location: left (3), middle (3) and right (3). The null hypothesis is that there is no difference among the three group means of cell growth (*i.e.*, the location of the bioreactor has no effect on cell growth). The alternative hypothesis is that at least one group means is different from others (*i.e.*, the location of the bioreactor has an effect on cell growth). The *p*-value from the repeated measures ANOVA is 0.9825 (>0.05), which means that the null hypothesis cannot be rejected at a 5% significance level, *i.e.*, there is no significant difference in cell growth by the location of the bioreactor in S3.

The above statistical analyses clearly confirm that the S3 delivered consistent growth conditions across all nine reactor systems, which is the prerequisite for reliable screening. In this way, three strains can be screened together, each with triplicates, therefore significantly expediting the screening process.

3.2) Methanotroph screening

Figure 2(a) displays growth profiles of the seven methanotrophs and their corresponding modified Gompertz (4Z) model fits. **Figure 2(a)** shows that the modified Gompertz model was able to capture the different growth patterns exhibited by different methanotroph strains adequately, indicating that it is reasonable to use the few model parameters to evaluate different strains. The maximum growth rate, delay time and carrying capacity of each methanotrophs are plotted in **Figures 2(b) – 2(d)**, respectively. All model parameters are also listed in Supplementary Material **Table S1** with the selected strains in bold.

[Insert Figure 2 here].

Based on the strain's maximum growth rate, delay time and carrying capacity, *Methylomonas sp*. LW13, *Methylosarcina fibrata*, and *Methylococcus capsulatus* were selected as candidates for the coculture-pair screening. As shown in **Figure 2**, these strains exhibited fast growth, short delay time on diluted AD digestate and achieved high biomass when reached stationary phase. It is worth noting that in a separate study, *M. sp. LW 13* and *M. fibrata* were the dominate methanotroph strains isolated from stream sediment and an anaerobic digester, respectively (Kim et al., 2018)(Kim et al., 2018).

Among the methanotrophs examined, *Methylomonas methanica* S1 exhibited the highest maximum growth rate (0.225 ± 0.021 1/hr). Despite its fast growth rate, it was not

chosen as a candidate for coculture screening due to the following considerations. M*ethylomonas* strains are known to produce extracellular polymeric substance (EPS) under stress (Wang et al., 2021)(Wang et al., 2021). In our experiment, 24 hours into the screening, the culture broth of *M. methanica* S1 was noticeably more viscous than other methanotrophs. The increased viscosity usually causes increased mass transfer resistance and increased energy demand for agitation. In addition, *M. methanica* S1 has a longer delay time and lower carrying capacity compared to the selected strains.

Although *Methylosinus trichosporium* OB3b has been studied as a versatile methanotroph with the potential for producing bioplastic precursors (Nguyen et al., 2020; Tays et al., 2018; Zhang et al., 2017), its modest growth rate and long delay time (4 – 50 times longer than the selected candidates) precluded it from further study. Nevertheless, its versatility in copper-deficient conditions, like other Type II methanotrophs, may be incentive to use it for different AD applications (Tays et al., 2018).

3.2.1) Microalga screening

Figure 2(e) plots the growth profiles of the five microalgae on 10% digestate and their corresponding modified Gompertz model fits. All microalgal species exhibited robust growth on wastewater with minimum delay, and the modified Gompertz model captured the growth pattern of different species very well, with adjusted R^2 values over 0.98. The maximum growth rate, delay time and carrying capacity of each microalgal species are plotted in **Figures 2(f) – 2(h)**, respectively. All model parameters are also listed in Supplementary Material **Table S1** with the selected strains in bold.

Chlorella sorokiniana and *Scenedesmus dimorphus* were selected as candidates for the coculture screening due to their rapid and robust growth on wastewater. *C. sorokiniana* and *S. dimorphus* exhibited the highest maximum growth rates and shortest delay times among all microalgal strains. *C. sorokiniana* also exhibited the second highest carrying capacity.

Figure 2(e) suggests that all microalgae screened are good candidates for wastewater treatment, while the specific applications would dictate which microalgae to select. For example, *C. vulgaris* exhibited the slowest maximum growth rate, but its high lipid content and high carrying capacity may be desirable for producing biofuel precursors or single-cell protein (Taziki et al., 2015; Wollmann et al., 2019). In addition, all five microalgal species exhibited relatively small delay times, indicating their tolerance to the inhibitors in the diluted AD digestate.

3.2.2) Coculture screening

The growth profiles of the six coculture pairs and their corresponding Gompertz model fits are shown in **Figure 3(a) – 3(f)**. The maximum growth rate, delay time and carrying capacity of the cocultures are plotted in **Figures 3(g) – 3(i)**, with all model

parameters listed in Supplementary Material **Table S1**. In general, the modified Gompertz model adequately captures the growth profiles of all the coculture pairs, with adjusted R^2 values higher than 0.99, except for *M. fibrata – C. sorokiniana* which has a slightly lower adjusted R^2 (0.97). This suggests that for the coculture pairs, the same set of Gompertz model parameters can accurately capture the dynamics of the coculture growth from inoculation till stationary phase. In other words, a good Gompertz fitting suggests that there are no significant growth dynamic changes (such as different metabolic interactions) happening during the coculture growth, and the coculture could be viewed as a "combined" monoculture that maintains the same growth dynamics throughout the batch experiment.

It is important to note that the cocultures were grown on synthetic biogas which contains no O_2, so the methanotroph in the coculture must rely on the oxygen produced by the microalgae to grow. In addition, although each screening vessel contains the same amount of nutrients, the light availability for the microalgae in the coculture can be different from its microalgae monoculture due to self-shading effect from the methanotrophs. Therefore, it can be misleading to directly compare the maximum growth rate of a coculture to the summation of the maximum growth rates of its monoculture components. To examine the differences between the coculture and its monoculture components, we plotted the growth profiles of the monocultures in a coculture on the same plot in **Figure 3(a) – 3(f)**. **Figure 3** suggests that all six coculture pairs screened are suitable for integrated biogas valorization and nutrient recovery, while *M. capsulatus – C. sorokiniana* exhibited the highest maximum growth rate and very short delay time.

[insert Figure 3 here]

The limiting factor in the screening experiment was the nutrient supply as carbon substrate was supplied through continuous gas bubbling. In addition, the growth of the methanotroph in a coculture was limited by the amount of oxygen produced by the microalgae. Therefore, the final biomass production from the coculture is expected to be somewhere between the final biomass of its monocultures, provided that there are no additional metabolic interactions within the coculture beyond exchange of O_2/CO_2, and there is no significant change in biomass composition. In other words, if the coculture biomass deviates significantly from its monocultures, it indicates that there may be significant interspecies interaction that change the biomass composition and/or growth dynamics.

Figure 3 clearly shows that the coculture pairs of *M. capsulatus – S. dimorphus* and *M. fibrata – C. sorokiniana* didn't follow this expectation, as their final biomass production significantly surpassed both of its monoculture components. However, the growth dynamics of *M. capsulatus – S. dimorphus* is quite different from that of *M. fibrata – C. sorokiniana*. As discussed in the following paragraph, for *M. fibrata – C. sorokiniana*, there were some changes in the growth dynamics that happened in the coculture after 40 hours

of cultivation; while for *M. capsulatus – S. dimorphus*, whatever changes caused by the cocultivation happened very early on, and the same set of the model parameters captured the complete coculture trajectory very well. Although unknown, the existence of interspecies interactions between *M. capsulatus* and *S. dimorphus* is also supported by the significantly reduced delay time (0.0031 ± 0.0018 hr. for the coculture, 4.7001 ± 2.1170 hr. for *M. capsulatus* and 2.2980 ± 0.8290 hr. for *S. dimorphus*). It is interesting to note that the delay time for *M. fibrata – C. sorokiniana* was much longer than both monocultures (4.8130 ±0.4157 hr for the coculture, 2.9869 ± 1.2675 hr for *M. fibrata* and 1.1412 ± 0.2034 hr for *C. sorokiniana*), indicating potential inhibitive effects at the beginning of cocultivation.

To explain why the Gompertz model fitting for *M. fibrata – C. sorokiniana* had lower adjusted R^2, in **Figure 4** we compare two sets of Gompertz model fits for *M. fibrata – C. sorokiniana* and *M. capsulatus – C. sorokiniana*. The solid lines are model fits using all growth data, while the dotted lines are model fits using the first 60 hours of data. The plot inserts provide the details for the initial period of experiment. For *M. capsulatus – C. sorokiniana*, the two model fits agree well with each other, suggesting the same set of parameters can adequately capture the complete growth trajectory. On the other hand, there is a large discrepancy between the two model fits for *M. fibrata – C. sorokiniana*, suggesting that there were some significant changes in the coculture after around 60 hours.

Interspecies interactions and symbiotic relationships within a community are known to exhibit dynamic shifts under different environmental conditions, which contribute to the resilience and robustness of the microbial community (Orland et al., 2019; Spor et al., 2011). This is confirmed in our research on a methanotroph-cyanobacteria coculture pair, which showed that in addition to the exchange of O_2 and CO_2, there exist other metabolic cross-feedings including metabolites in the central carbon metabolic network, nitrogen sources and a range of amino acids (Badr et al., 2024, 2022). In particular, the exchange of nitrogen source and amino acids (septically glutamate) were established after 48 hours of the cocultivation. Nutrient limitation may be the trigger for the growth dynamic change that happened around 60 hours, as the N and P measurements confirmed that both nutrients were depleted by 48 hours. It should be noted that nutrient limitation also occurred 48 hours into the monoculture screening experiment for both *M. fibrata* and *C. sorokiniana* while no changing dynamics were observed in the monoculture. Compared to its monocultures, the higher degree of freedom and a larger pool of genes provided by the coculture could enable enhanced robustness against nutrient limitation, which could explain the different growth dynamics observed in the latter half of the experiment and significantly higher final biomass concentration. The maximum growth rate and delay time for *M. fibrata – C. sorokiniana* coculture reported in **Figure 3** and Supplementary Material **Table S1** were the ones obtained by using the first 60 hours of data, as they were associated with initial unlimited growth of the coculture.

[insert Figure 4 here]

Figure 3 also shows that the same methanotroph strain paired with *C. sorokiniana* exhibited a higher maximum growth rate than that paired with *S. dimorphus*. This is likely because the *C. sorokiniana* monoculture grew faster than the *S. dimorphus* monoculture. Since the growth of the methanotroph in the coculture is limited by the oxygen produced by the microalgae, the slower growth of the microalgae usually indicates slower oxygenation, therefore slower growth of the methanotroph in the coculture. However, it is interesting to note that despite the lowest maximum growth rate exhibited by *M. capsulatus – S. dimorphus*, this coculture had the shortest delay time and produced the second highest final biomass at the end. The significantly reduced delay time of *M. capsulatus – S. dimorphus* suggests that there exist some emergent synergistic interactions that enable the coculture to enter the growth phase immediately. These synergistic interactions, potentially metabolic cross-feedings, persisted throughout the experiment, which enabled the accumulation of the 2nd highest coculture biomass at the end of the experiment.

3.3. Temperature effects on *M. capsulatus* and its coculture

Temperature is a key factor that affects the growth performance of monocultures and cocultures. It could also alter the interspecies interactions within a coculture. While most microalgae screened in this study grow optimally between 25°C - 30°C (Pawlita-Posmyk et al., 2018), the thermotolerant *M. capsulatus* grows optimally at 37 - 45°C (Bedekar et al., 2023; Oshkin et al., 2021) which is much higher than the optimal temperature for microalgae. To select a temperature that enables coculture screening, we first conducted experiments to examine the temperature effect on the methanotroph and its cocultures.

Prior literature has different optimal growth temperature of *M. capsulatus*, either 37°C or 42°C (Bedekar et al., 2023; Henard et al., 2018; Soni et al., 1998). One study examined the biomass composition of *M. capsulatus* cultivated under different temperatures. When cultivated on ammonium, the primary nitrogen source in 10% digestate, *M. capsulatus* Bath has a higher protein content and lower lipid content when cultivated at 37°C than when cultivated at 42°C (Bedekar et al., 2023). Based on these findings, four temperatures were tested in this work for *M. capsulatus* cultivated on 10% digestate: 30°C, 37°C, 42°C and 47°C. **Figure 5(a)** shows the growth profiles of *M. capsulatus* under different temperatures and their corresponding Gompertz model fits. The model parameters are shown in **Figure 5(b) – (d)**. On 10% digestate, *M. capsulatus* exhibited the highest maximum growth rate at 42°C, followed by 47°C and 37°C. This is expected as the thermostability and activity of enzymes in *M. capsulatus* are optimal around 45°C. When deviating from the optimal temperature, enzyme activities decrease, and cell growth slows down. Although capable of growing on defined medium at 30°C, *M. capsulatus* showed no growth on 10% digestate, likely due to the additional stress caused by the inhibitors in the digestate.

[insert Figure 5 here]

Considering the optimal growth temperature of both methanotroph and microalgae, 30 °C and 37 °C were tested on the cocultures containing *M. capsulatus*. **Figure 5(e)** plots the growth profiles of the coculture pairs (*M. capsulatus* - *S. dimorphus* and *M. capsulatus* - *C. sorokiniana*) under different temperatures and their corresponding Gompertz model fits. The model parameters are plotted in **Figure 5(f) – 5(h)**.

Although *M. capsulatus – S. dimorphus* exhibited similar maximum growth rates and delay times at 30 and 37 °C, the cocultures composition were drastically different as shown in the microscopic images of the final liquid sample (**Figure 6**). At 30°C, the coculture was dominated by healthy *S. dimorphus* cells with a small but significant presence of *M. capsulatus* in the coculture. The presence of *M. capsulatus* in the coculture was further supported by the UV-Vis wavelength scans of the coculture samples (Supplementary Material **Figure S4**), which displayed a negative slope across the wavelengths, a signature of methanotroph biomass. This result suggests that when co-cultivated with *S. dimorphus* on 10% digestate, *M. capsulatus* exhibited better growth than its monoculture which showed no growth, possibly due to some synergistic effects within the coculture. At 37°C, the coculture was dominated by *M. capsulatus*, with few significantly enlarged *S. dimorphus* cells (possibly due to the stress caused by higher temperature). As there was no oxygen in the feeding gas, the prevalence of *M. capsulatus* at 37 °C suggests that the few *S. dimorphus* cells were able to provide the oxygen needed to support methanotroph growth.

[insert Figure 6 here]

For *M. capsulatus – C. sorokiniana*, the coculture exhibited different maximum growth rates and different composition at different temperatures. At 30 °C, the coculture was dominated by microalgae with almost no methanotroph, which was supported by the UV-Vis wavelength scan of the coculture sample as the negative slope was barely present. This result suggests that at 30 °C there was no clearly synergistic effect between *M. capsulatus* and *C. sorokiniana*. At 37 °C, a balanced methanotroph and microalgae populations were present in the coculture, and the coculture exhibited the highest growth rate with slightly reduced delay time (2.9097 ± 0.2536 hr) compared to the monoculture of *M. capsulatus* (4.7001 ± 2.1170 hr). It is not clear if this reduction in delay time was due to the short delay time of *C. sorokiniana* (1.1412 ± 0.2034 hr) or potential synergistic effect within the coculture.

Conclusions:

Driven by the need for an affordable and effective system that can efficiently screen different methanotroph-microalgae cocultures, we developed a microbial species screening system that can deliver tightly controlled growth conditions across nine parallel bioreactor systems, including temperature, pH, agitation rate, gas feed composition and

rate, and light intensity. The consistent growth condition among the nine bioreactor systems was validated by growing *C. sorokiniana* on 10% digestate, where the strain cultured in different bioreactor systems exhibited uniform growth performance across all nine vessels.

To screen methanotroph-microalgae cocultures for integrated biogas valorization and nutrient recovery, seven methanotrophs and five microalgae were selected as candidate strains based on their feasibility for wastewater treatment. As it has been shown that the removal of nutrients from the liquid broth is linearly related to the strain's biomass production before nutrients are depleted, we used growth performance as the key metric to assess different strains. In our screening experiment, different strains exhibited different delay times and growth characteristics on 10% digestate. As a result, directly comparing different growth profiles for performance assessment can be subjective and lead to biased conclusions. To consistently and quantitatively assess different strains for their suitability for the desired application, we developed a modified Gompertz model to fit the growth data and used a few model parameters to assess different strains. Specifically, we mainly consider their maximum growth rate (which indicates how efficiently the strain recovers nutrients and produces biomass), delay time (which indicates how robust the strain is in tolerating the inhibitors in wastewater) and carrying capacity (how much biomass could be generated given limited nutrient) when selecting top monoculture candidates for coculture screening. Based on these metrics, three methanotrophs (*M. sp.* LW13, *M. fibrata*, and *M. capsulatus*) and two microalgae (*C. sorokiniana* and *S. dimorphus*) were selected for coculture screening. All six coculture pairs screened demonstrated robust growth of both species in the coculture, demonstrating their feasibility for the desired application. Among the six coculture pairs, two of them exhibited different behavior from other cocultures, suggesting significant interspecies interactions. In addition to coculture screening, the system was applied to examine the effect of temperature on monoculture and coculture growth. The results showed that the interspecies interactions within a coculture can be drastically different at different temperatures.

Although long-term stability tests were not performed in this work, in our previous work, we have tested the coculture of *M. capsulatus – C. sorokiniana* for the integrated biogas valorization and nutrient recovery under continuous operation. Some of the continuous runs lasted over five weeks and the coculture demonstrated stable performance under varying nutrient loads (due to varying dilution rate) (Roberts, 2020). In addition, we have found that *M. capsulatus – C. sorokiniana* can tolerate H_2S up to 3,000 ppm in biogas, and both strains use/prefer ammonia as the nitrogen source (Roberts et al., 2020). Although these results were obtained for one coculture pair only, we expect other coculture pairs to exhibit similar robustness in continuous operations, provided that they demonstrate robust growth in batch screening experiments.

Data statement

All the experimental data, MATLAB scripts and figures can be found on GitHub: https://github.com/AU-Wang-He-Group/S3_Data_Analysis

Glossary:

AD – Anaerobic digestion / anaerobic digestor
EPS – Extracellular Polymeric Substance
LED – Light emitting diode
NaOH – Sodium hydroxide
HCl – Hydrochloric acid
S3 – Species Screening System
CH_4 – Methane (gas)
CO_2 – Carbon dioxide (gas)
O_2 – Diatomic oxygen (gas)
N_2 – Diatomic nitrogen (gas)
H_2S – Hydrogen sulfide
NH_3 – Ammonia
MFC – Mass flow controller

Acknowledgements

The authors would like to thank Prof. Mary Lidstrom (University of Washington) for providing several methanotroph strains; Dr. Michael Guarnieri (National Renewable Energy Laboratory) for providing several microalgae strains; and Mr. Brian Boswell (Columbus Water Works) for providing wastewater samples.

Author contributions

LPM: Methodology, Software, Formal analysis, Investigation, Writing – original Draft; QPH: Conceptualization, Formal analysis, Writing – review & editing, Funding acquisition; JW: Conceptualization, Methodology, Formal analysis, Writing – original draft, Writing – review & editing, Supervision, Funding acquisition.

Funding sources

This work was supported by the U.S. Department of Education GAANN Program (Award Number P200A210047), U.S. Department of Energy, Office of Science, Genomic Science Program (Award Number DE-SC0019181), U.S. Department of Agriculture (Award Number 2023-67021-39643), National Science Foundation (Award Number NSF-CBET-2331602), and Alabama Department of Economic and Community Affairs (Award Number ADECA-1ARDEF22 03).

Table 1: Methanotrophs, microalgae, and cocultures screened. The defined medium for preculturing is listed, along with the abiotic conditions controlled by the S3 during screening

	Species	Shorthand (Meth Type)	Defined Medium (Preculture)	Temp (S3)	Gas Feed (S3)	Light Intensity (S3)	Agitation (S3)	pH (S3)
Methano-trophs	*Methylosarcina fibrata*	Fib (I)	DSMZ Medium 921[a]	30°C	30 vol% CH_4 20 vol% O_2 2 vol% CO_2 48 vol% N_2 (0.22vvm)	-	300 rpm	7.0
	Methylosarcina quisquiliarum	QQ (I)						
	Methylosarcina lacus LW14^T	LW14T (I)						
	Methylomonas sp. LW13	LW13 (I)	Modified AMS[b]					
	Methylomonas methanica S1	S1 (I)						
	Methylosinus trichosporium OB3b	OB3b (II)						
	Methylococcus capsulatus (Bath)	Cap (X)		37°C				
Microalgae	*Chlorella kessleri*	Kess	N8[c]	28°C	2 vol% CO_2 98 vol% N_2 (0.22vvm)	180 µE/m^2/s		
	Chlorella sorokiniana	Soro						
	Chlorella vulgaris	Vulg						
	Scenedesmus dimorphus	Dim	Proteose[d]					
	Scenedesmus obliquus	Obli						
Cocultures	*M. capsulatus* + *S. dimorphus*	Cap + Dim	-	30°C & 37°C	4 vol% CH4 2 vol% CO2 94 vol%N2 (0.18vvm)	180 µE/m^2/s		
	M. capsulatus + *C. sorokiniana*	Cap + Soro						
	M. fibrata + *S. dimorphus*	Fib + Dim		30°C				
	M. fibrata + *C. sorokiniana*	Fib + Soro						
	M. sp. LW13 + *S. dimorphus*	LW13 + Dim						
	M. sp. LW13 + *C. sorokiniana*	LW13 + Soro						

References:

AlSayed, A., Fergala, A., Eldyasti, A., 2018. Sustainable biogas mitigation and value-added resources recovery using methanotrophs intergrated into wastewater treatment plants. Rev Environ Sci Biotechnol 17, 351–393.

Angelidaki, I., Ellegaard, L., 2003. Codigestion of manure and organic wastes in centralized biogas plants. Appl Biochem Biotechnol 109, 95–105.

Badr, K., He, Q.P., Wang, J., 2024. Probing interspecies metabolic interactions within a synthetic binary microbiome using genome-scale modeling. Microbiome Research Reports 3, N-A.

Badr, K., He, Q.P., Wang, J., 2022. A novel semi-structured kinetic model of methanotroph-photoautotroph cocultures for biogas conversion. Chemical Engineering Journal 431, 133461. https://doi.org/https://doi.org/10.1016/j.cej.2021.133461

Badr, K., Whelan, W., Peter He, | Q, Wang, J., 2021. Fast and easy quantitative characterization of methanotroph-photoautotroph cocultures. Biotechnol Bioeng 118, 703–714. https://doi.org/10.1002/bit.27603

Bedekar, A.A., Deewan, A., Jagtap, S.S., Parker, D.A., Liu, P., Mackie, R.I., Rao, C. V, 2023. Transcriptional and metabolomic responses of Methylococcus capsulatus Bath to nitrogen source and temperature downshift. Front Microbiol 14, 1259015.

Girden, E.R., 1992. ANOVA: Repeated measures. sage.

Gupta, S.K., Ansari, F.A., Shriwastav, A., Sahoo, N.K., Rawat, I., Bux, F., 2016. Dual role of Chlorella sorokiniana and Scenedesmus obliquus for comprehensive wastewater treatment and biomass production for bio-fuels. J Clean Prod 115, 255–264.

Henard, C.A., Franklin, T.G., Youhenna, B., But, S., Alexander, D., Kalyuzhnaya, M.G., Guarnieri, M.T., 2018. Biogas biocatalysis: methanotrophic bacterial cultivation, metabolite profiling, and bioconversion to lactic acid. Front Microbiol 9, 2610.

Kim, J., Kim, D.D., Yoon, S., 2018. Rapid isolation of fast-growing methanotrophs from environmental samples using continuous cultivation with gradually increased dilution rates. Appl Microbiol Biotechnol 102, 5707–5715.

Kip, N., van Winden, J.F., Pan, Y., Bodrossy, L., Reichart, G.-J., Smolders, A.J.P., Jetten, M.S.M., Damsté, J.S.S., den Camp, H.J.M.O., 2010. Global prevalence of methane oxidation by symbiotic bacteria in peat-moss ecosystems. Nat Geosci 3, 617–621. https://doi.org/https://doi.org/10.1038/ngeo939

Liu, K.E., Valentine, A.M., Qiu, D., Edmondson, D.E., Appelman, E.H., Spiro, T.G., Lippard, S.J., 1997. Characterization of a Diiron (III) Peroxo Intermediate in the Reaction Cycle of Methane Monooxygenase Hydroxylase from Methylococcus capsulatus (Bath) J. Am. Chem. Soc. 1995, 117, 4997− 4998. J Am Chem Soc 119, 11134–11135.

Milucka, J., Kirf, M., Lu, L., Krupke, A., Lam, P., Littmann, S., Kuypers, M.M.M., Schubert, C.J., 2015. Methane oxidation coupled to oxygenic photosynthesis in anoxic waters. ISME J. https://doi.org/https://doi.org/10.1038/ismej.2015.12

Nasir, I.M., Mohd Ghazi, T.I., Omar, R., 2012. Anaerobic digestion technology in livestock manure treatment for biogas production: a review. Eng Life Sci 12, 258–269.

Nguyen, D.T.N., Lee, O.K., Lim, C., Lee, J., Na, J.-G., Lee, E.Y., 2020. Metabolic engineering of type II methanotroph, Methylosinus trichosporium OB3b, for production of 3-hydroxypropionic acid from methane via a malonyl-CoA reductase-dependent pathway. Metab Eng 59, 142–150.

Orland, C., Emilson, E.J.S., Basiliko, N., Mykytczuk, N.C.S., Gunn, J.M., Tanentzap, A.J., 2019. Microbiome functioning depends on individual and interactive effects of the environment and community structure. ISME J 13, 1–11. https://doi.org/https://doi.org/10.1038/s41396-018-0230-x

Oshkin, I.Y., Danilova, O. V, But, S.Y., Miroshnikov, K.K., Suleimanov, R.Z., Belova, S.E., Tikhonova, E.N., Kuznetsov, N.N., Khmelenina, V.N., Pimenov, N. V, 2021. Expanding characterized diversity and the pool of complete genome sequences of Methylococcus species, the bacteria of high environmental and biotechnological relevance. Front Microbiol 12, 756830.

Patel, S.K.S., Kalia, V.C., Lee, J.-K., 2023. Integration of biogas derived from dark fermentation and anaerobic digestion of biowaste to enhance methanol production by methanotrophs. Bioresour Technol 369, 128427.

Pawlita-Posmyk, M., Wzorek, M., Płaczek, M., 2018. The influence of temperature on algal biomass growth for biogas production, in: MATEC Web of Conferences. EDP Sciences, p. 04008.

Qi, Y., Beecher, N., Finn, M., 2013. Biogas Production and Use at Water Resource Recovery Facilities in the United States. Water Environment Federation.

Raghoebarsing, A.A., Smolders, A.J.P., Schmid, M.C., Rijpstra, W.I.C., Wolters-Arts, M., Derksen, J., Jetten, M.S.M., Schouten, S., Damsté, J.S.S., Lamers, L.P.M., others, 2005. Methanotrophic symbionts provide carbon for photosynthesis in peat bogs. Nature 436, 1153–1156. https://doi.org/https://doi.org/10.1038/nature03802

Rasouli, Z., Valverde-Pérez, B., D'Este, M., De Francisci, D., Angelidaki, I., 2018. Nutrient recovery from industrial wastewater as single cell protein by a co-culture of green microalgae and methanotrophs. Biochem Eng J 134, 129–135. https://doi.org/https://doi.org/10.1016/j.bej.2018.03.010

Roberts, N., Hilliard, M., He, Q.P., Wang, J., 2020. A microalgae-methanotroph coculture is a promising platform for fuels and chemical production from wastewater. Front Energy Res 8, 230. https://doi.org/https://doi.org/10.3389/fenrg.2020.563352

Roberts, N.R.M., 2020. A scalable and sustainable wastewater treatment technology using a methanotroph-microalga co-culture. Auburn University.

Soni, B.K., Conrad, J., Kelley, R.L., Srivastava, V.J., 1998. Effect of temperature and pressure on growth and methane utilization by several methanotrophic cultures, in: Biotechnology for Fuels and Chemicals. Springer, pp. 729–738.

Spor, A., Koren, O., Ley, R., 2011. Unravelling the effects of the environment and host genotype on the gut microbiome. Nat Rev Microbiol 9, 279–290. https://doi.org/https://doi.org/10.1038/nrmicro2540

Tays, C., Guarnieri, M.T., Sauvageau, D., Stein, L.Y., 2018. Combined effects of carbon and nitrogen source to optimize growth of proteobacterial methanotrophs. Front Microbiol 9, 2239.

Taziki, M., Ahmadzadeh, H., Murry, M.A., 2015. Growth of Chlorella vulgaris in high concentrations of nitrate and nitrite for wastewater treatment. Curr Biotechnol 4, 441–447.

Tjørve, K.M.C., Tjørve, E., 2017. The use of Gompertz models in growth analyses, and new Gompertz-model approach: An addition to the Unified-Richards family. PLoS One 12, e0178691.

Topper, P.A., Graves, R.E., Richard, T., 2006. The fate of nutrients and pathogens during anaerobic digestion of dairy manure. Lehman (PA): Penn State University. College of Agricultural Science, Cooperative Extension Bulletin G 71.

U.S. Environmental Protection Agency, 2024. Inventory of U.S. Greenhouse Gas Emissions and Sinks: 1990-2022.

Wang, D.-H., Zhu, M.-Y., Lian, S.-J., Zou, H., Fu, S.-F., Guo, R.-B., 2022. Conversion of renewable biogas into single-cell protein using a combined microalga-and methane-oxidizing bacterial system. ACS ES&T Engineering 2, 2317–2325.

Wang, H., Zheng, Y., Zhu, B., Zhao, F., 2021. In situ role of extracellular polymeric substances in microbial electron transfer by Methylomonas sp. LW13. Fundamental Research 1, 735–741.

Wang, J., He, Q.P., 2023. Microalgae-methanotroph cocultures for nutrient recovery from wastewater, in: Lens, P.N.L., Khandelwal, A. (Eds.), Algal Systems for Resource Recovery from Waste and Wastewater. IWA Publishing, London, pp. 103–125.

Ward, N., Larsen, Ø., Sakwa, J., Bruseth, L., Khouri, H., Durkin, A.S., Dimitrov, G., Jiang, L., Scanlan, D., Kang, K.H., 2004. Genomic insights into methanotrophy: the complete genome sequence of Methylococcus capsulatus (Bath). PLoS Biol 2, e303.

Wollmann, F., Dietze, S., Ackermann, J., Bley, T., Walther, T., Steingroewer, J., Krujatz, F., 2019. Microalgae wastewater treatment: Biological and technological approaches. Eng Life Sci 19, 860–871.

Zhang, B., Cai, C., Zhou, Y., 2023. Iron and nitrogen regulate carbon transformation in a methanotroph-microalgae system. Science of the Total Environment 904, 166287.

Zhang, T., Zhou, J., Wang, X., Zhang, Y., 2017. Coupled effects of methane monooxygenase and nitrogen source on growth and poly-β-hydroxybutyrate (PHB) production of Methylosinus trichosporium OB3b. Journal of Environmental Sciences 52, 49–57.

Zwietering, M.H., Jongenburger, I., Rombouts, F.M., Van't Riet, K., 1990. Modeling of the bacterial growth curve. Appl Environ Microbiol 56, 1875–1881.

FIGURES

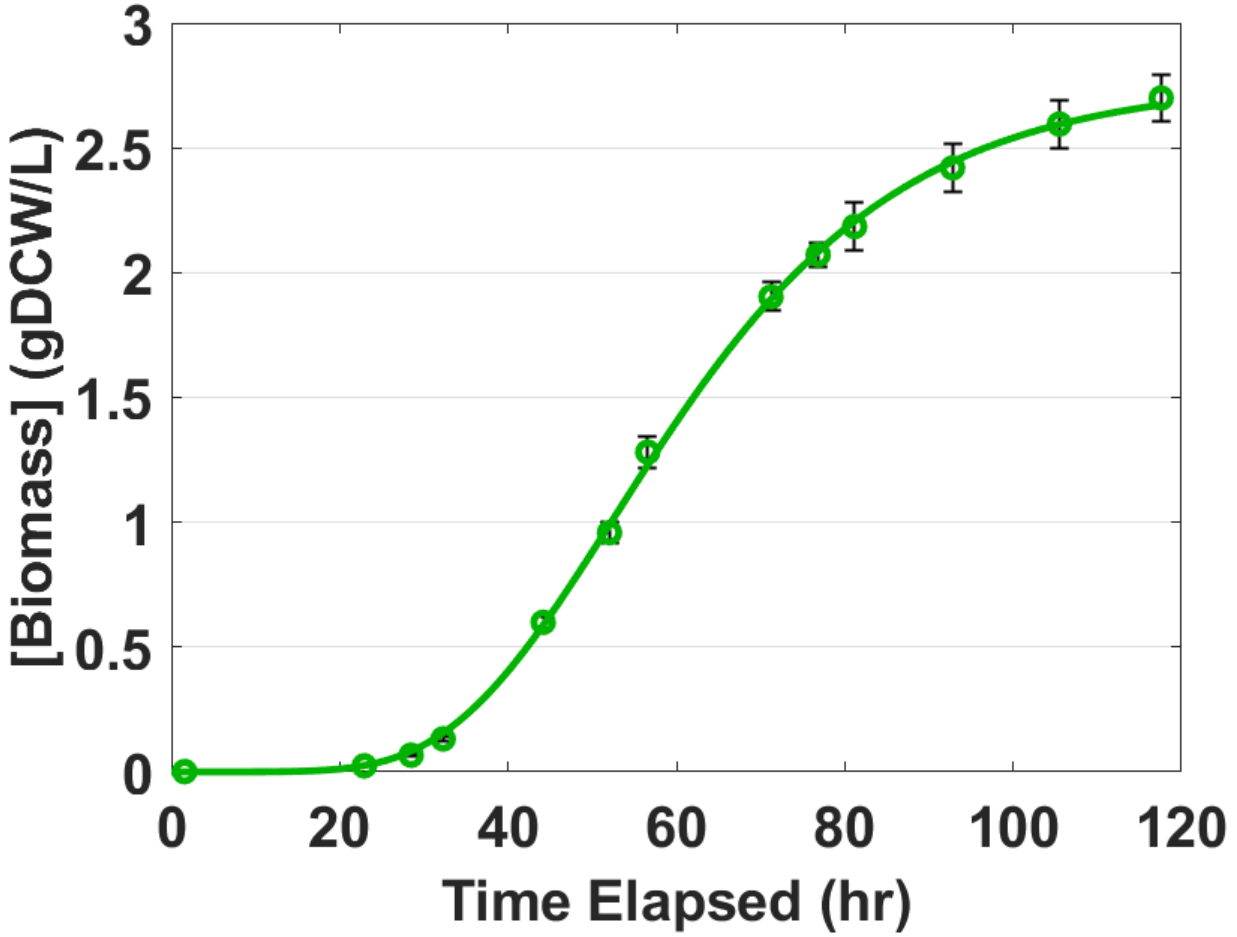

Figure 1: Photograph of S3 and growth plot of *C. sorokiniana* on diluted AD across all nine vessels at the same conditions: 28°C, 300rpm, 180 µE/m^2/s, pH: 7.0, Gas: 2 vol% CO_2 in N_2 at 0.22 vvm

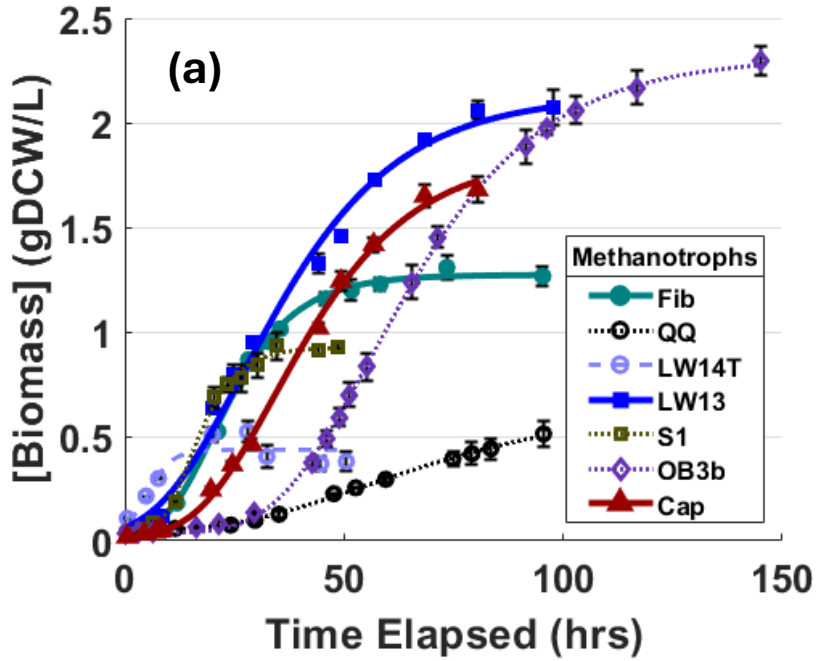
(a)
[Biomass] (gDCW/L)
Time Elapsed (hrs)
Methanotrophs
Fib
QQ
LW14T
LW13
S1
OB3b
Cap

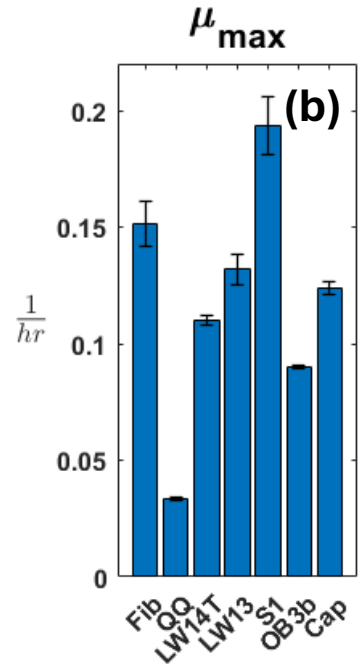
μ_{max}
(b)
$\frac{1}{hr}$
Fib
QQ
LW14T
LW13
S1
OB3b
Cap

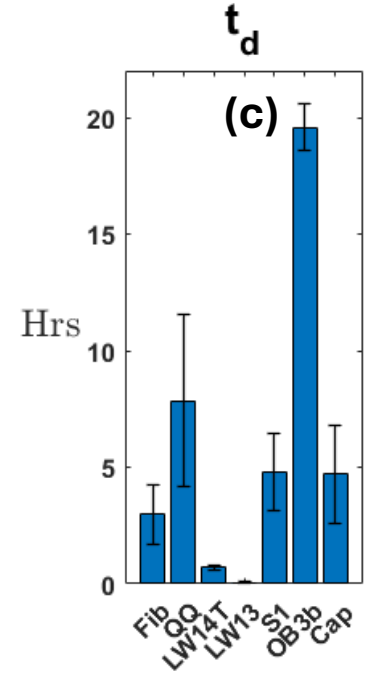
t_d
(c)
Hrs
Fib
QQ
LW14T
LW13
S1
OB3b
Cap

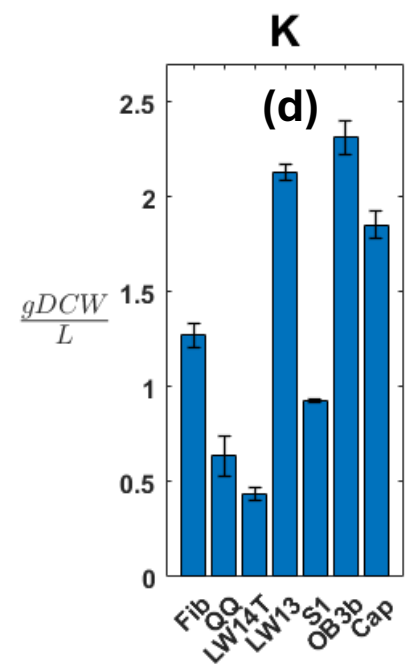
K
(d)
$\frac{gDCW}{L}$
Fib
QQ
LW14T
LW13
S1
OB3b
Cap

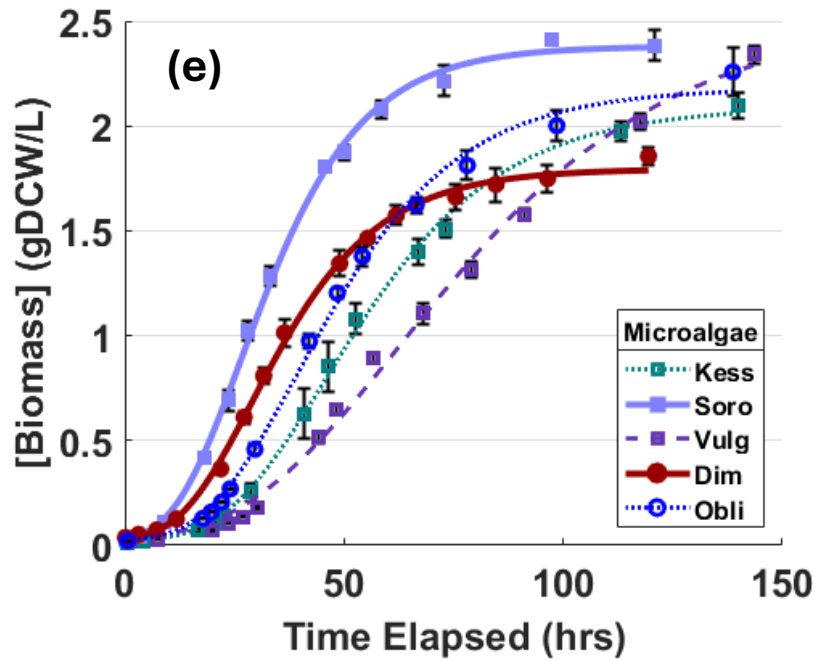
(e)
[Biomass] (gDCW/L)
Time Elapsed (hrs)
Microalgae
Kess
Soro
Vulg
Dim
Obli

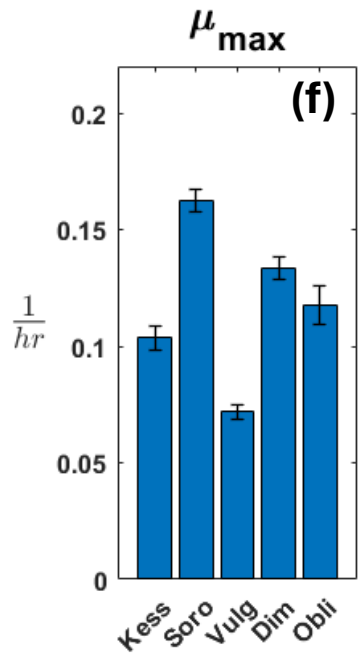
μ_{max}
(f)
$\frac{1}{hr}$
Kess
Soro
Vulg
Dim
Obli

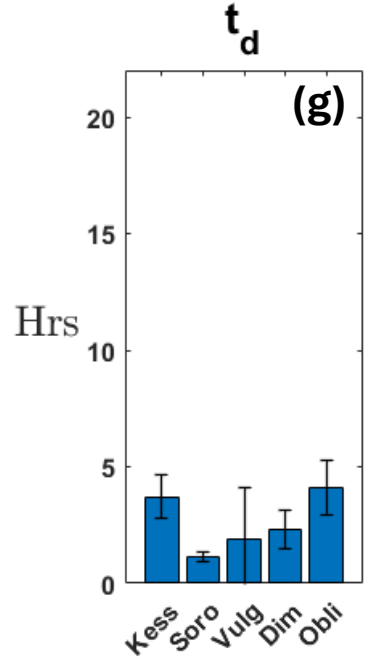
t_d
(g)
Hrs
Kess
Soro
Vulg
Dim
Obli

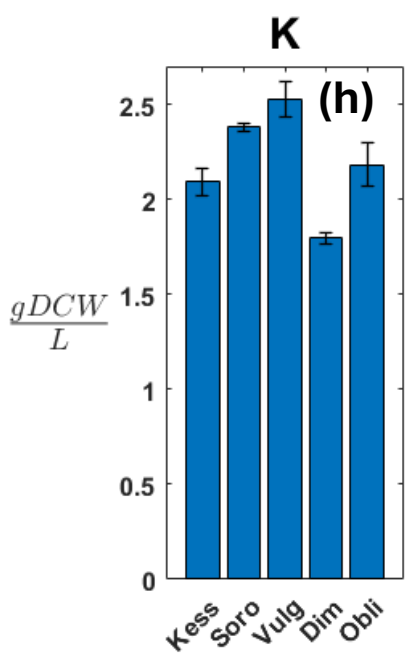
K
(h)
$\frac{gDCW}{L}$
Kess
Soro
Vulg
Dim
Obli

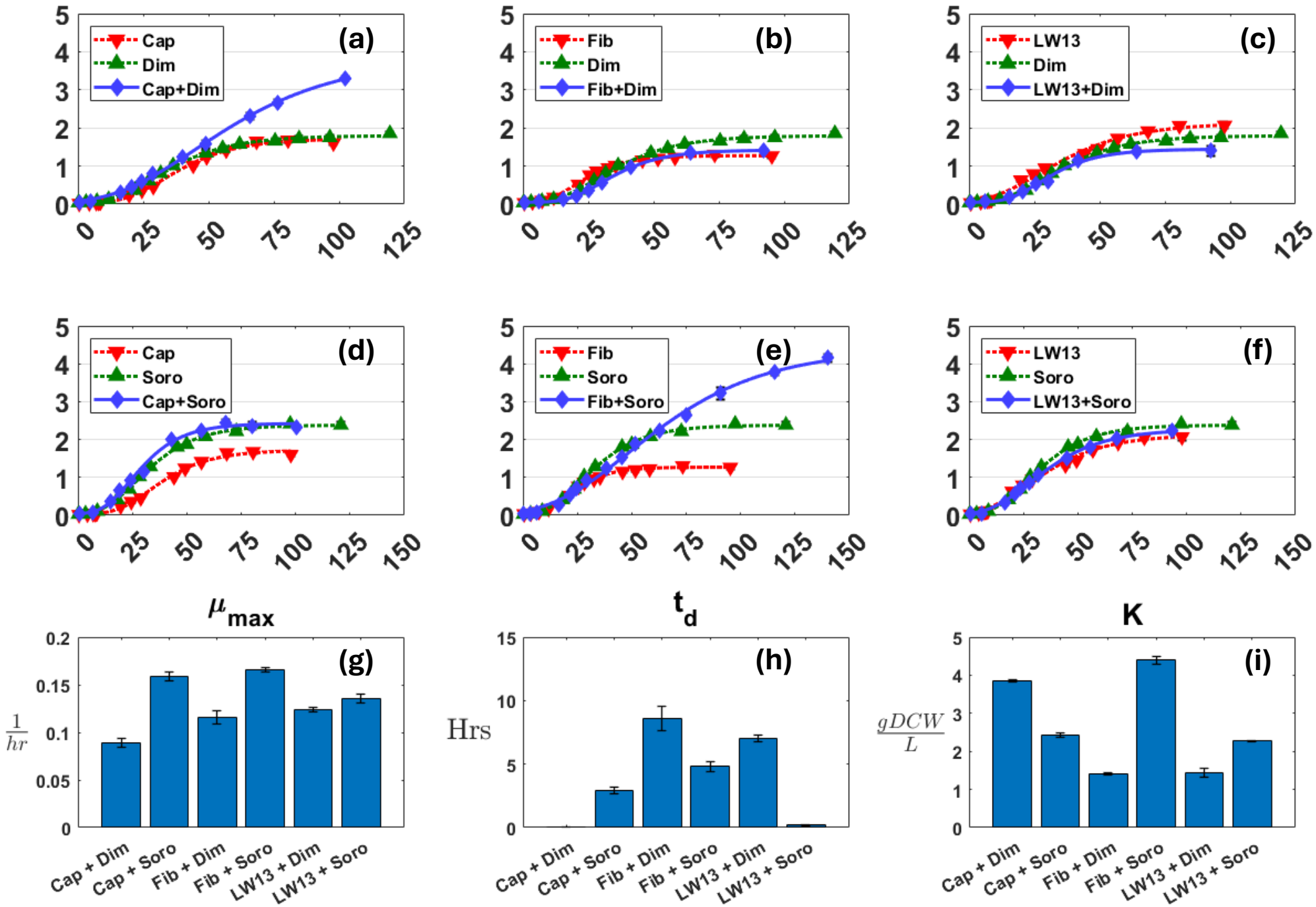
(a)
Cap
Dim
Cap+Dim
(b)
Fib
Dim
Fib+Dim
(c)
LW13
Dim
LW13+Dim
(d)
Cap
Soro
Cap+Soro
(e)
Fib
Soro
Fib+Soro
(f)
LW13
Soro
LW13+Soro
μmax
1/hr
(g)
td
Hrs
(h)
K
gDCW/L
(i)
Cap + Dim
Cap + Soro
Fib + Dim
Fib + Soro
LW13 + Dim
LW13 + Soro

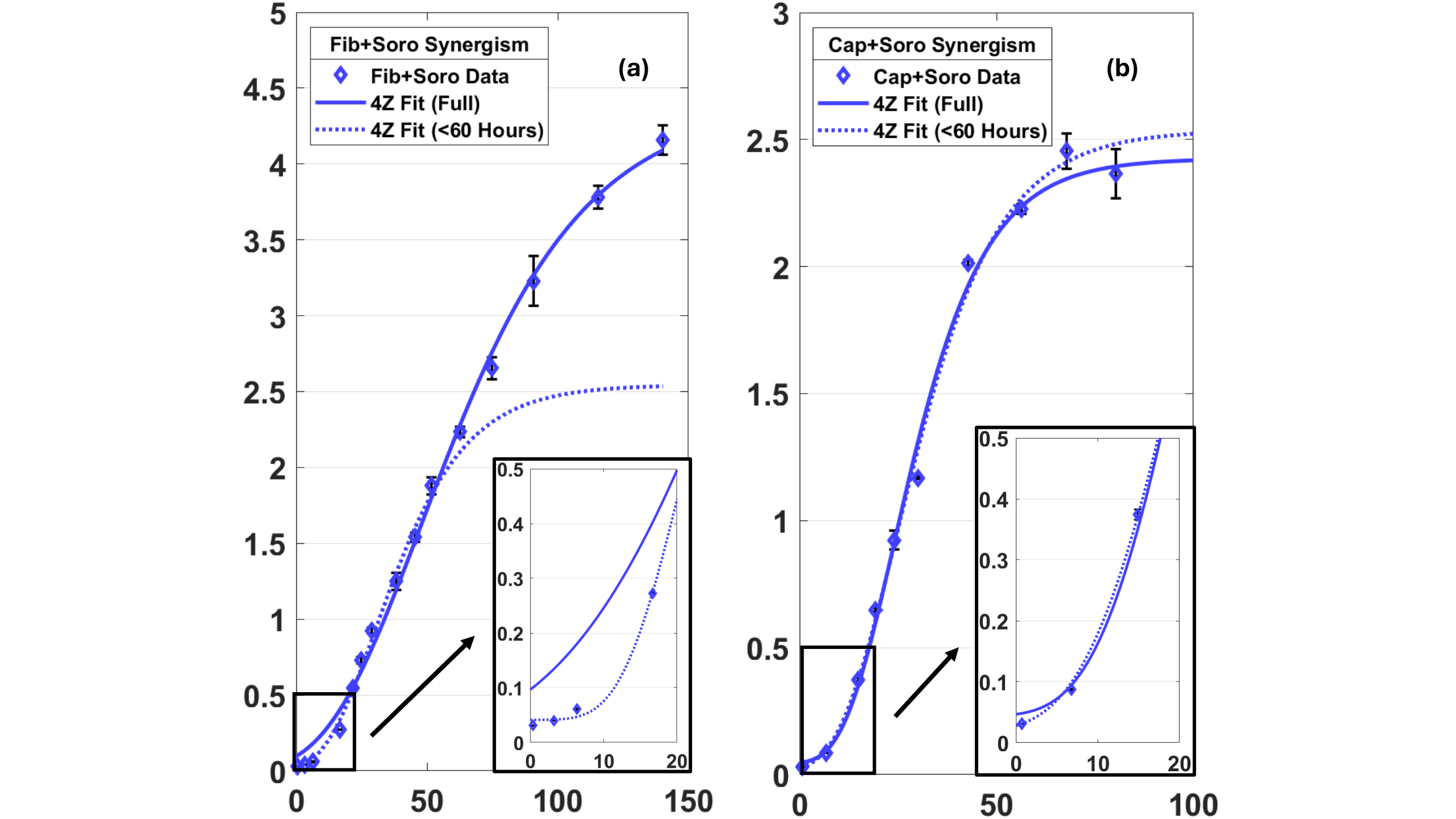
Fib+Soro Synergism
Fib+Soro Data
4Z Fit (Full)
4Z Fit (<60 Hours)
(a)
Cap+Soro Synergism
Cap+Soro Data
4Z Fit (Full)
4Z Fit (<60 Hours)
(b)

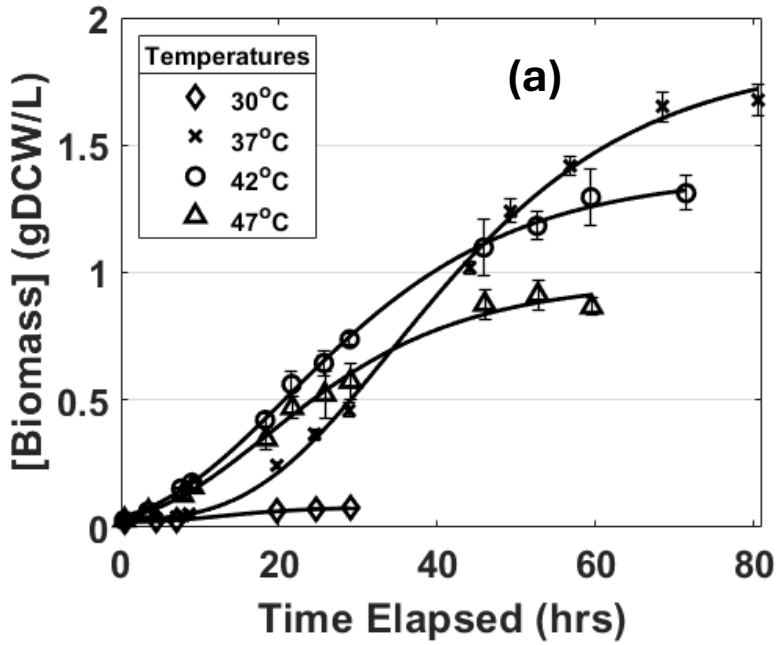
Temperatures
30°C
37°C
42°C
47°C
(a)
[Biomass] (gDCW/L)
Time Elapsed (hrs)

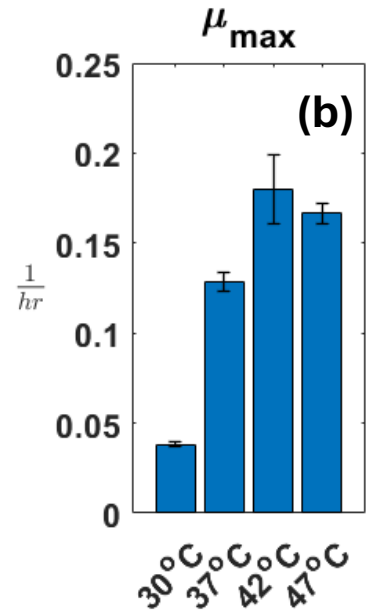
μmax
(b)
1/hr

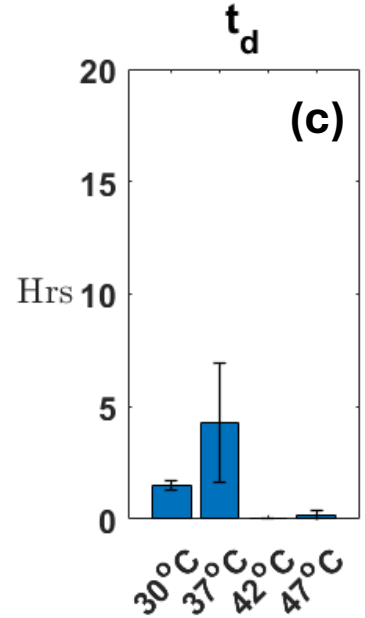
td
(c)
Hrs

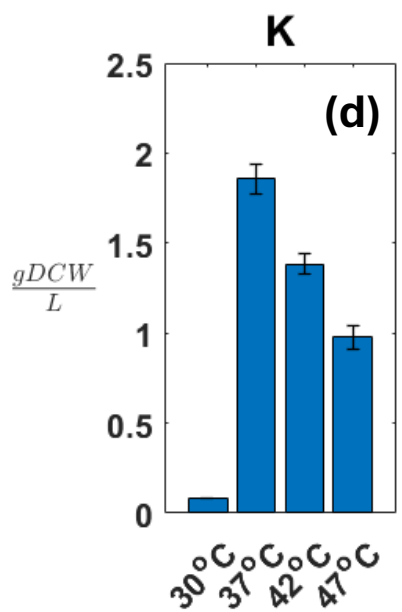
K
(d)
gDCW/L

(a)

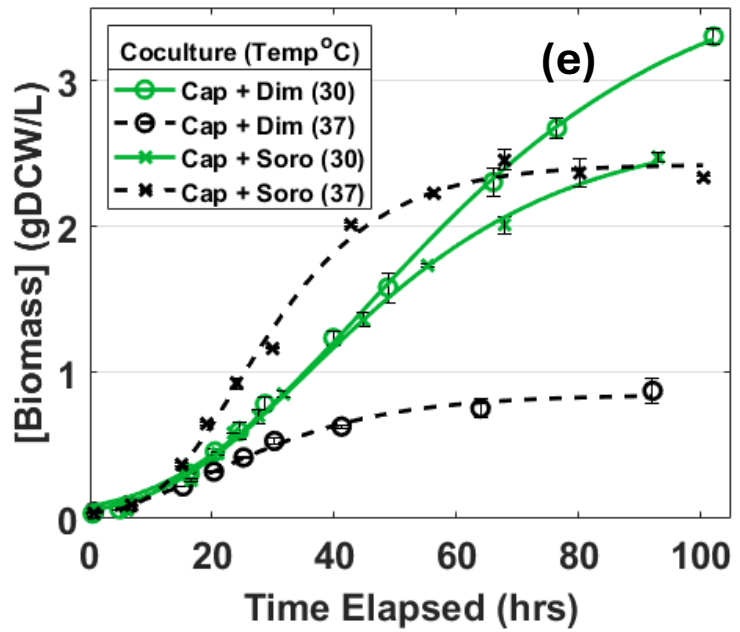
Coculture (Temp°C)
Cap + Dim (30)
Cap + Dim (37)
Cap + Soro (30)
Cap + Soro (37)
(e)
[Biomass] (gDCW/L)
Time Elapsed (hrs)

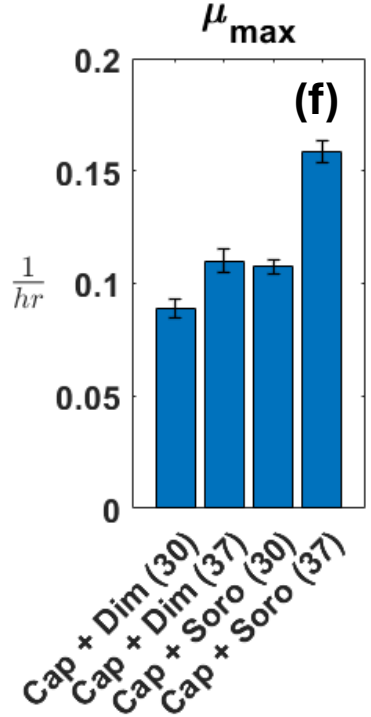
μmax
(f)
1/hr
Cap + Dim (30)
Cap + Dim (37)
Cap + Soro (30)
Cap + Soro (37)

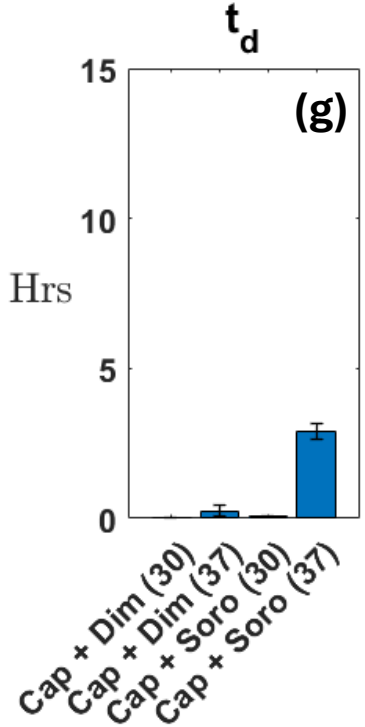
td
(g)
Hrs
Cap + Dim (30)
Cap + Dim (37)
Cap + Soro (30)
Cap + Soro (37)

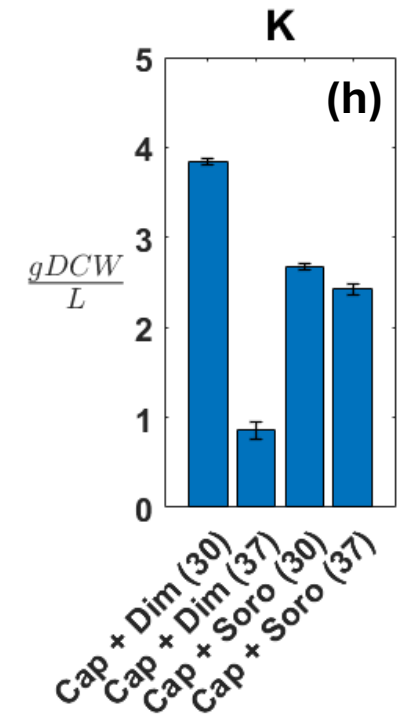
K
(h)
gDCW/L
Cap + Dim (30)
Cap + Dim (37)
Cap + Soro (30)
Cap + Soro (37)

Figure 6: Microscope pictures of *M. capsulatus* cocultures at the late exponential phase of growth. The red circles highlight the presence of *M. capsulatus* in the *S. dimorphus* coculture at 30°C

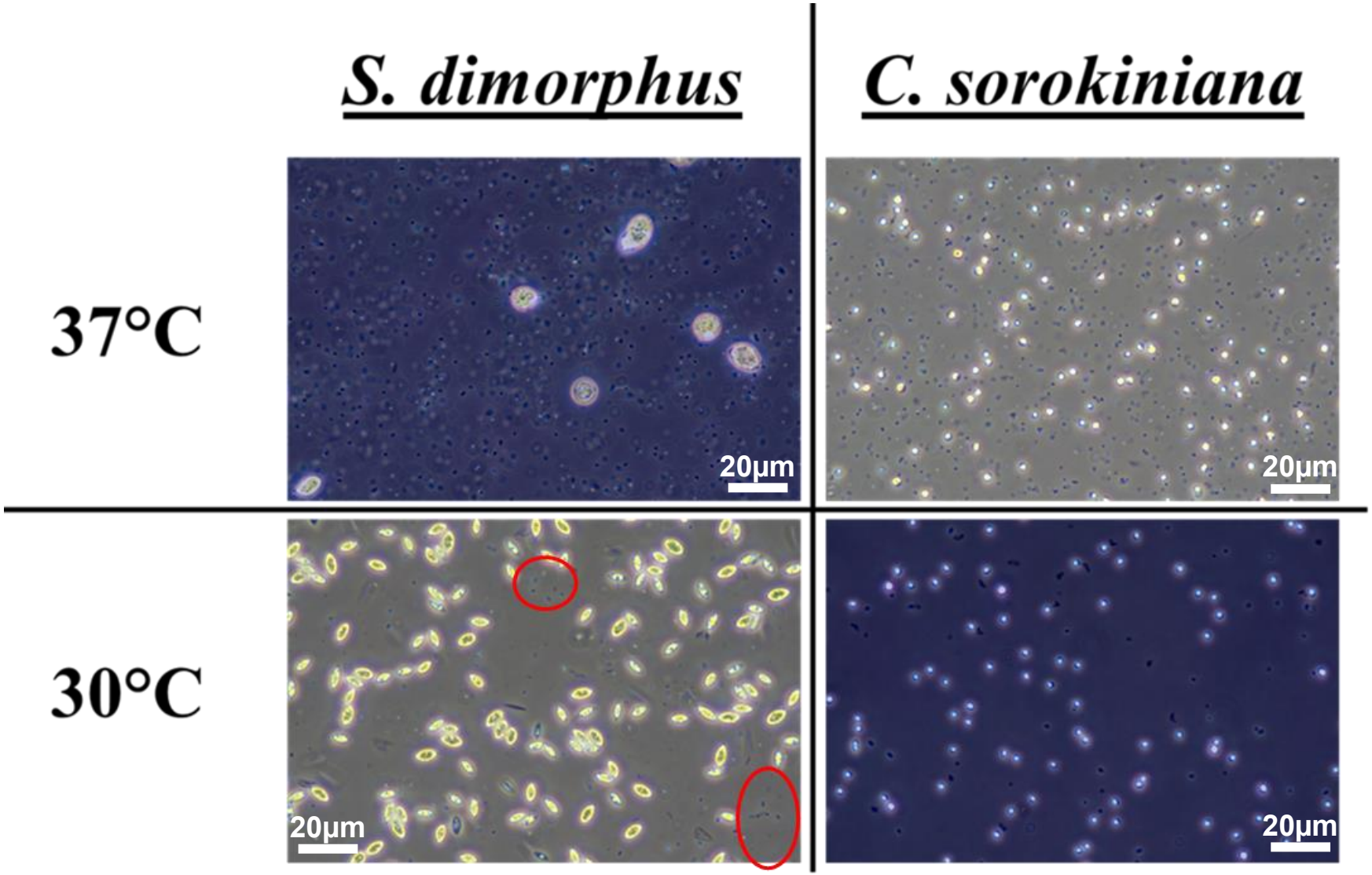

Table 1: Methanotrophs, microalgae, and MPC's screened. The defined medium for preculturing is listed, along with the settings for each of the six abiotic factors controlled by the S3.

	Species	Shorthand (Meth Type)	Defined Medium (Preculture)	Temperature (S3)	Gas Feed (S3)	Light Intensity (S3)	Agitation (S3)	pH (S3)
Methanotrophs	*Methylosarcina fibrata*	Fib (I)	DSMZ Medium 921[a]	30°C	30vol% CH_4 20vol% O_2 2vol% CO_2 48vol% N_2 (0.22vvm)	-	300 rpm	7.0
	Methylosarcina quisquiliarum	QQ (I)						
	Methylosarcina lacus LW14^T	LW14T (I)						
	Methylomonas sp. LW13	LW13 (I)	Modified AMS[b]					
	Methylomonas methanica S1	S1 (I)						
	Methylosinus trichosporium OB3b	OB3b (II)						
	Methylococcus capsulatus (Bath)	Cap (X)		37°C				
Microalgae	*Chlorella kessleri*	Kess	N8[c]	28°C	2vol% CO_2 98vol% N_2 (0.22vvm)	180 uE/m^2/s		
	Chlorella sorokiniana	Soro						
	Chlorella vulgaris	Vulg						
	Scenedesmus dimorphus	Dim	Proteose[d]					
	Scenedesmus obliquus	Obli						
MPC	*M. capsulatus* + *S. dimorphus*	Cap + Dim	-	30°C	4% CH4 2% CO2 94%N2 (0.18vvm)	180 uE/m2/s		
	M. capsulatus + *C. sorokiniana*	Cap + Soro		37°C				
	M. fibrata + *S. dimorphus*	Fib + Dim		30°C				
	M. fibrata + *C. sorokiniana*	Fib + Soro						
	M. sp. LW13 + *S. dimorphus*	LW13 + Dim						
	M. sp. LW13 + *C. sorokiniana*	LW13 + Soro						

SUPPLEMENTAL FIGURES + TABLES

Figure S1: Vessel schematic for each of the nine S3 bioreactors.

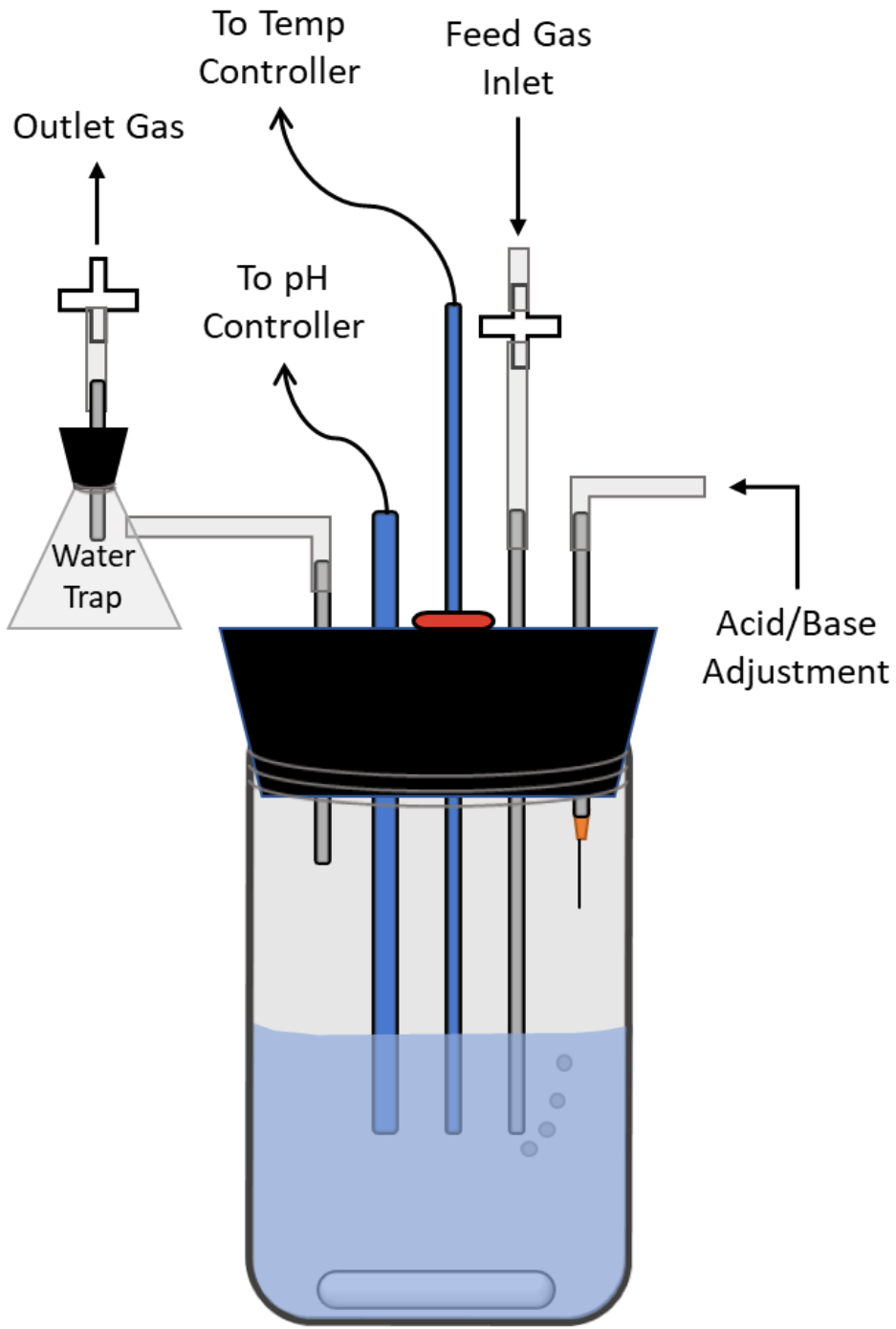

Figure S2: LED wall schematic for the S3

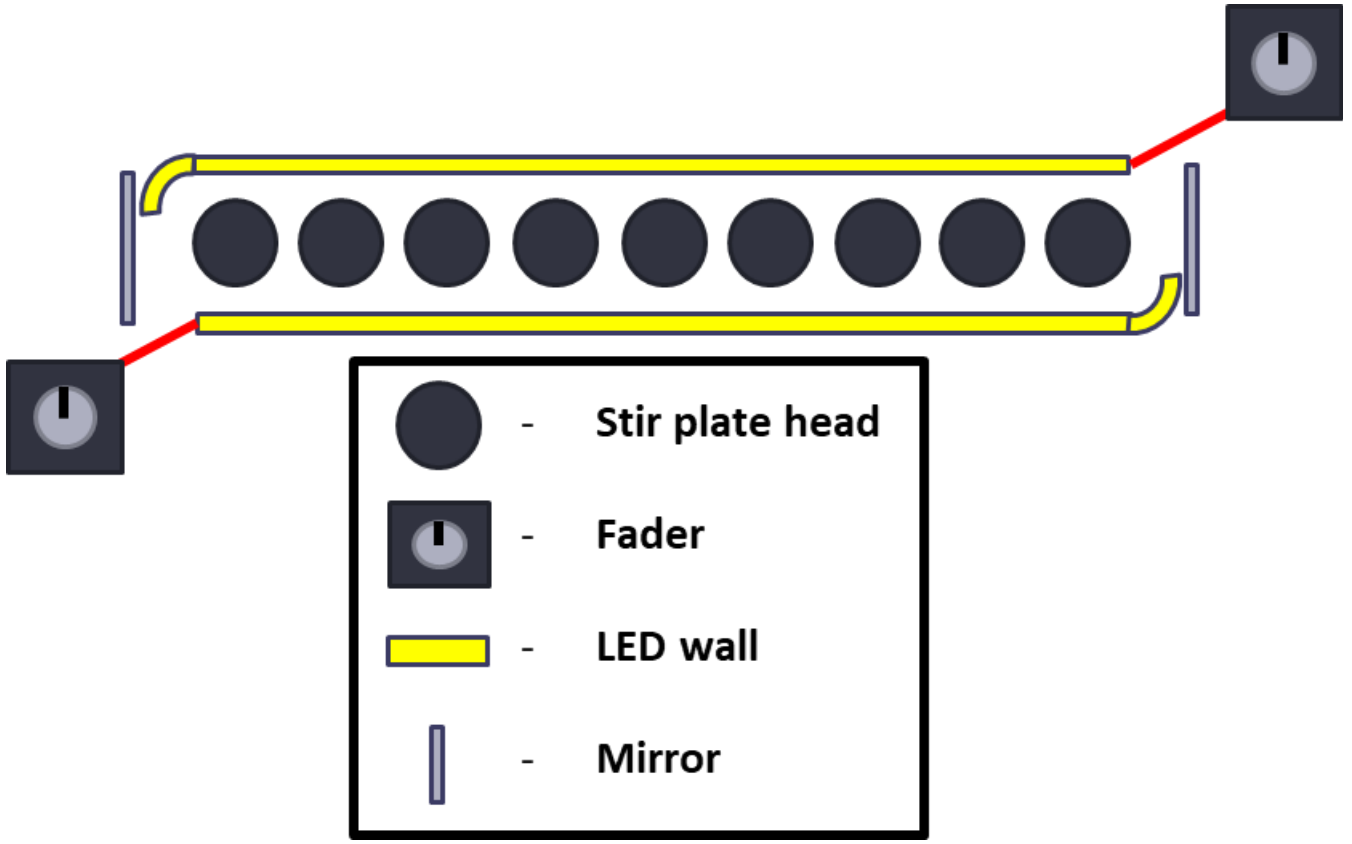

Figure S3: Gas feed schematic for supplying accurate gas feed rates and composition to each of the nine S3 vessels. Photographs of the mass flow controller (MFC) and variable-area flow meters are provided.

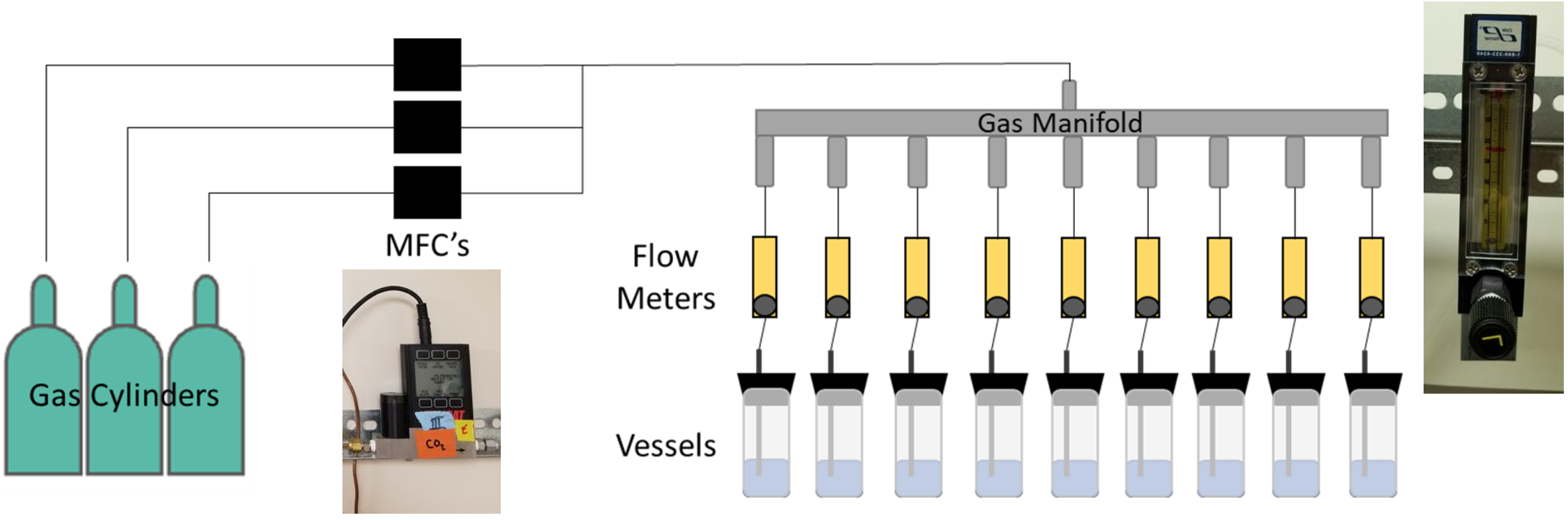

Figure S4: Dynamic UV-Vis wavelength scans from 400nm – 800nm of the *M. capsulatus* MPC's. The order of the plots matches *Figure* 6.

37°C

30°C

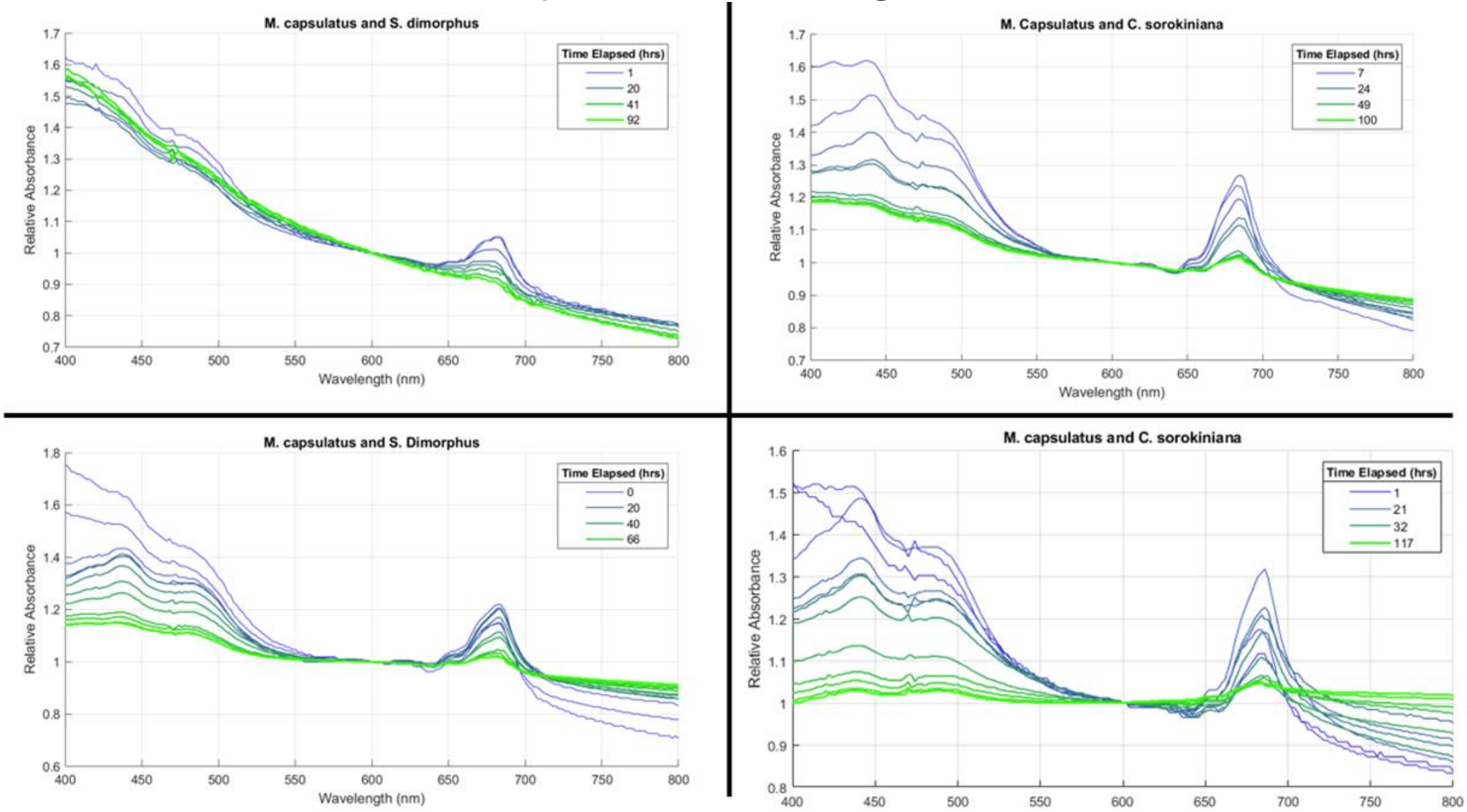

Table S1: Gompertz estimations for maximum growth rate, stationary biomass concentration, lag time, and delay time for methanotrophs, microalgae, and MPC's. Bolded methanotrophs and microalgae were selected for coculture analysis and include their monikers used in the MPC's.

	Species or MPC	Maximum Growth Rate (1/hr)	Stationary Biomass (gDCW/L)	Lag Time (hr)	Delay Time (hr)
Methanotrophs	***M. fibrata* (Fib)**	**0.1514 ± 0.0095**	**1.2731 ± 0.0638**	**9.3451 ± 0.7896**	**2.9869 ± 1.2675**
	M. quisquiliarum	0.0335 ± 0.0008	0.6353 ± 0.1094	24.0991 ± 5.1718	7.8412 ± 3.6778
	M. lacus LW14^T	0.1018 ± 0.0010	0.4357 ± 0.0294	2.4271 ± 0.2346	0.9096 ± 0.1454
	***M. sp.* LW13 (LW13)**	**0.1317 ± 0.0068**	**2.1300 ± 0.0452**	**7.4463 ± 0.4384**	**0.0395 ± 0.0343**
	M. methanica S1	0.1935 ± 0.0123	0.9270 ± 0.0051	8.5551 ± 1.0367	4.7721 ± 1.6462
	M. trichosporium OB3b	0.0899 ± 0.0009	2.3108 ± 0.0926	34.8201 ± 0.8970	19.5787 ± 1.0225
	***M. capsulatus* (Cap)**	**0.1236 ± 0.0028**	**1.8526 ± 0.0750**	**16.7974 ± 0.9851**	**4.7001 ± 2.1170**
Microalgae	*C. kessleri*	0.1035 ± 0.0051	2.0913 ± 0.0731	23.3121 ± 2.1488	3.7228 ± 0.9086
	***C. sorokiniana* (Soro)**	**0.1623 ± 0.0049**	**2.3806 ± 0.0209**	**11.2040 ± 0.4062**	**1.1412 ± 0.2034**
	C. vulgaris	0.0718 ± 0.0032	2.5249 ± 0.0939	27.2225 ± 0.4554	1.8982 ± 2.1973
	***S. dimorphus* (Dim)**	**0.1336 ± 0.0050**	**1.7963 ± 0.0302**	**12.5872 ± 0.3351**	**2.2980 ± 0.8290**
	S. obliquus	0.1175 ± 0.0084	2.1834 ± 0.1106	18.7629 ± 0.6759	4.0900 ± 1.1901
MPC's	Cap + Dim	0.0889 ± 0.0043	3.8455 ± 0.0323	13.7594 ± 0.3897	0.0031 ± 0.0018
	Cap + Soro	0.1587 ± 0.0050	2.4246 ± 0.0576	11.3223 ± 0.2012	2.9097 ± 0.2536
	Fib + Dim	0.1158 ± 0.0071	1.4226 ± 0.0298	16.9795 ± 0.7040	8.5765 ± 0.9494
	Fib + Soro	0.1657 ± 0.0026*	4.3930 ± 0.1071	12.9096 ± 0.7653	4.8130 ± 0.4157*
	LW13 + Dim	0.1240 ± 0.0020	1.4415 ± 0.1055	14.8933 ± 0.1788	7.0377 ± 0.2626
	LW13 + Soro	0.1360 ± 0.0047	2.2708 ± 0.0225	9.3815 ± 0.3156	0.2075 ± 0.0450

* Fib + Soro maximum growth rates and delay times shown using first 60 hours of data

Table S2: Gompertz estimations for maximum growth rate, stationary biomass concentration, lag time, and delay time for the *M. capsulatus* cocultures at 30C and 37C

	Microalga and Temp	Maximum Growth Rate (1/hr)	Stationary Biomass (gDCW/L)	Lag Time (hr)	Delay Time (hr)
***M. capsulatus* Cocultures**	Soro (30°C)	0.1064 ± 0.0031	2.6857 ± 0.0388	11.2965 ± 0.2758	0.0530 ± 0.0289
	Dim (30°C)	0.0895 ± 0.0043	3.8377 ± 0.0318	13.9060 ± 0.3841	0.0029 ± 0.0012
	Soro (37°C)	0.1612 ± 0.0053	2.4250 ± 0.0576	11.2539 ± 0.2032	2.7367 ± 0.2544
	Dim (37°C)	0.1170 ± 0.0131	0.8500 ± 0.0920	4.3928 ± 0.4825	0.1905 ± 0.0982